LI
LABORATORY INVESTIGATION
THE BASIC AND TRANSLATIONAL PATHOLOGY RESEARCH JOURNAL
VOLUME 99 | SUPPLEMENT 1 | MARCH 2019

USCAP 2019

ABSTRACTS

DERMATOPATHOLOGY
(466-505)

USCAP 108TH ANNUAL MEETING

UNLOCKING YOUR INGENUITY

MARCH 16-21, 2019

National Harbor, Maryland
Gaylord National Resort & Convention Center

Published by
SPRINGER NATURE
www.ModernPathology.org

USCAP Creating a Better Pathologist
AN OFFICIAL JOURNAL OF THE UNITED STATES AND CANADIAN ACADEMY OF PATHOLOGY

EDUCATION COMMITTEE

Jason L. Hornick, Chair
Rhonda K. Yantiss, Chair, Abstract Review Board and Assignment Committee
Laura W. Lamps, Chair, CME Subcommittee
Steven D. Billings, Interactive Microscopy Subcommittee
Shree G. Sharma, Informatics Subcommittee
Raja R. Seethala, Short Course Coordinator
Ilan Weinreb, Subcommittee for Unique Live Course Offerings
David B. Kaminsky (Ex-Officio)
Aleodor (Doru) Andea
Zubair Baloch
Olca Basturk
Gregory R. Bean, Pathologist-in-Training
Daniel J. Brat
Ashley M. Cimino-Mathews
James R. Cook
Sarah M. Dry
William C. Faquin
Carol F. Farver
Yuri Fedoriw
Meera R. Hameed
Michelle S. Hirsch
Lakshmi Priya Kunju
Anna Marie Mulligan
Rish Pai
Vinita Parkash
Anil Parwani
Deepa Patil
Kwun Wah Wen, Pathologist-in-Training

ABSTRACT REVIEW BOARD

Benjamin Adam
Michelle Afkhami
Narasimhan (Narsi) Agaram
Rouba Ali-Fehmi
Ghassan Allo
Isabel Alvarado-Cabrero
Christina Arnold
Rohit Bhargava
Justin Bishop
Jennifer Boland
Elena Brachtel
Marilyn Bui
Shelley Caltharp
Joanna Chan
Jennifer Chapman
Hui Chen
Yingbei Chen
Benjamin Chen
Rebecca Chernock
Beth Clark
James Conner
Alejandro Contreras
Claudiu Cotta
Timothy D'Alfonso
Farbod Darvishian
Jessica Davis
Heather Dawson
Elizabeth Demicco
Suzanne Dintzis
Michelle Downes
Daniel Dye
Andrew Evans
Michael Feely
Dennis Firchau
Larissa Furtado
Anthony Gill
Ryan Gill
Paula Ginter
Tamara Giorgadze
Raul Gonzalez
Purva Gopal
Anuradha Gopalan
Jennifer Gordetsky
Rondell Graham
Alejandro Gru
Nilesh Gupta
Mamta Gupta
Krisztina Hanley
Douglas Hartman
Yael Heher
Walter Henricks
John Higgins
Mai Hoang
Mojgan Hosseini
Aaron Huber
Peter Illei
Doina Ivan
Wei Jiang
Vickie Jo
Kirk Jones
Neerja Kambham
Chiah Sui (Sunny) Kao
Dipti Karamchandani
Darcy Kerr
Ashraf Khan
Rebecca King
Michael Kluk
Kristine Konopka
Gregor Krings
Asangi Kumarapeli
Alvaro Laga
Cheng-Han Lee
Zaibo Li
Haiyan Liu
Xiuli Liu
Yan-Chun Liu
Tamara Lotan
Anthony Magliocco
Kruti Maniar
Jonathan Marotti
Emily Mason
Jerri McLemore
Bruce McManus
David Meredith
Anne Mills
Neda Moatamed
Sara Monaco
Atis Muehlenbachs
Bita Naini
Dianna Ng
Tony Ng
Ericka Olgaard
Jacqueline Parai
Yan Peng
David Pisapia
Alexandros Polydorides
Sonam Prakash
Manju Prasad
Peter Pytel
Joseph Rabban
Stanley Radio
Emad Rakha
Preetha Ramalingam
Priya Rao
Robyn Reed
Michelle Reid
Natasha Rekhtman
Michael Rivera
Michael Roh
Andres Roma
Avi Rosenberg
Esther (Diana) Rossi
Peter Sadow
Safia Salaria
Steven Salvatore
Souzan Sanati
Sandro Santagata
Anjali Saqi
Frank Schneider
Jeanne Shen
Jiaqi Shi
Wun-Ju Shieh
Gabriel Sica
Deepika Sirohi
Kalliopi Siziopikou
Lauren Smith
Sara Szabo
Julie Teruya-Feldstein
Gaetano Thiene
Khin Thway
Rashmi Tondon
Jose Torrealba
Evi Vakiani
Christopher VandenBussche
Sonal Varma
Endi Wang
Christopher Weber
Olga Weinberg
Sara Wobker
Mina Xu
Shaofeng Yan
Anjana Yeldandi
Akihiko Yoshida
Gloria Young
Minghao Zhong
Yaolin Zhou
Hongfa Zhu
Debra Zynger

466 ALK Overexpression is Frequent and Relatively Specific for Merkel Cell Carcinoma Among Poorly Differentiated Neuroendocrine Carcinomas: A Finding of Diagnostic and Potential Therapeutic Import

Sumaya Al Rawi[1], Anthony Snow[2], Jason Hornick[3], Benjamin Darbro[4], Geraldine Pinkus[5], Andrew Bellizzi[1]
[1]University of Iowa Hospitals and Clinics, Iowa City, IA, [2]North Liberty, IA, [3]Brigham and Women's Hospital, Harvard Medical School, Boston, MA, [4]University of Iowa, Iowa City, IA, [5]Brigham and Women's Hospital, Boston, MA

Disclosures: Anthony Snow: None; Jason Hornick: None; Benjamin Darbro: None; Geraldine Pinkus: None; Andrew Bellizzi: None

Background: Anaplastic lymphoma kinase (ALK) overexpression due to translocation drives subsets of anaplastic large cell lymphoma (50%), inflammatory myofibroblastic tumor (60%), and lung adenocarcinoma (5%). We were surprised to see that the most recent NordiQC ALK immunohistochemistry (IHC) proficiency testing assessment included a positive Merkel cell carcinoma (MCC). Literature review revealed only two previous reports of ALK expression by MCC. It was initially fortuitously discovered on screening of multitissue tumor blocks with highly sensitive (HS)-ALK IHC. It was subsequently independently discovered by gene expression profiling. Results in only 58 MCCs and 12 small cell lung cancers have been reported to date.

Design: ALK IHC was performed using HS (D5F3) and standard (ALK1) clones on tissue microarrays of 42 MCCs and 31 and 21 poorly differentiated neuroendocrine carcinomas (PDNEC) of lung (L) and extrapulmonary visceral (EPV) origin. ALK break apart fluorescence in situ hybridization (FISH; Abbott Molecular) was performed on a subset (22 MCC, 10 L-PDNEC, 10 EPV-PDNEC). CK20 and TTF-1 IHC had been performed previously. IHC expression was evaluated for intensity (0-3+) and extent (0-100%) with an H-score (intensity*extent) calculated. McNemar and Mann-Whitney tests were used with $p<0.05$ considered significant.

Results: HS-ALK IHC was positive in 83% of MCCs with a mean (median) H-score of 189 (190); 14% of EPV-PDNECs (H-scores of 300, 145, and 33.3) and 3% of L-PDNECs (H-score 20) were positive. One of 4 CK20-negative MCCs was HS-ALK-positive (H-score 160). ALK1 IHC was negative in all cases. FISH failed to demonstrate evidence of translocation or amplification. HS-ALK and CK20 were similarly sensitive for a diagnosis of MCC and showed similar H-scores (both $p=0.19$). Results of HS-ALK, CK20, and TTF-1 IHC are compared in the Table.

	HS-ALK % Positive	Mean (Median) Positive H-score	CK20 % Positive	Mean (Median) Positive H-score	TTF-1 % Positive	Mean (Median) Positive H-score
MCC	83%	189 (190)	89%	213 (240)	3%	10 (10)
L-PDNEC	3%	20 (20)	7%	9 (9)	83%	200 (227)
EPV-PDNEC	14%	159 (145)	10%	192 (192)	43%	138 (190)

Conclusions: HS-ALK IHC is frequently positive in MCC and only rarely in other PDNECs. Positivity may suggest a diagnosis of MCC in occasional CK20-negative tumors. Given the FISH results (and the results of 2 prior studies describing the MCC mutational landscape), ALK overexpression appears to have an epigenetic cause. Given the efficacy of crizotinib, ALK may represent an attractive therapeutic target in this class of tumors.

467 Rapid Detection of BRAF and NRAS Mutations in Melanoma Using a Fully Automated System: a Comparison with Next Generation Sequencing

M. Rabie Al-Turkmani[1], Donald Green[2], Shaofeng Yan[3], Robert LeBlanc[2], Gregory Tsongalis[2]
[1]Dartmouth-Hitchcock Medical Center and Geisel School of Medicine at Dartmouth, Lebanon, NH, [2]Dartmouth-Hitchcock Medical Center, Lebanon, NH, [3]Hanover, NH

Disclosures: M. Rabie Al-Turkmani: None; Shaofeng Yan: None; Robert LeBlanc: None; Gregory Tsongalis: None

Background: Melanoma treatment has been revolutionized with the development of effective molecular and immune targeted therapies. Approximately one-half of advanced melanomas harbor a mutation in *BRAF*, with V600E being the most common mutation. *NRAS* mutations are found in 15 - 20% of melanomas and are typically associated with aggressive disease and poor outcomes. In this retrospective study, we evaluated *BRAF* and *NRAS* targeted mutation testing in melanoma specimens using a fully integrated, cartridge-based system that provides automated sample processing (deparaffinization, tissue digestion and DNA extraction) and real-time PCR-based mutation detection with all reagents included in a single-use cartridge.

Design: Twelve archived formalin-fixed paraffin-embedded (FFPE) melanoma tissue specimens were tested on the Idylla™ automated system (Biocartis, Belgium) using the NRAS-BRAF cartridges (Research Use Only). Among these samples, 5 had a mutation in *BRAF,* 4 had a mutation in *NRAS,* and 3 had no mutations in *BRAF* or *NRAS* as determined by previous next-generation sequencing (NGS) testing using the Ion AmpliSeq 50-gene Cancer Hotspot Panel v2 (Thermo Fisher Scientific). One 10 µm FFPE tissue section was used for each

run on the cartridge-based system and all cases met the system's minimum tumor requirement of 10%. Reproducibility and limit of detection were evaluated by testing commercial standards derived from human cell lines that have *BRAF* or *NRAS* mutations at 5% allele frequency.

Results: The cartridge-based system successfully detected mutations previously identified by NGS in all samples tested, including *BRAF* (V600E, V600K, V600R) and *NRAS* (G12C, G13R, Q61R) mutations. No mutations were detected in the wild-type samples. Analysis of the standard materials confirmed the expected sensitivity and results were reproducible. The system produced results quickly with a turnaround time of approximately 2 hours.

Conclusions: The described cartridge-based system offers rapid and reliable testing of clinically actionable *NRAS* and *BRAF* mutations in melanoma directly from FFPE tissue sections. Its simplicity and ease of use compared to other available molecular techniques make it suitable for small centers that lack highly trained staff and infrastructure. It can also complement NGS at larger diagnostic centers by providing rapid turnaround times that benefit time-sensitive decisions in the care of patients with melanoma.

468 B7-H3 Expression in Merkel Cell Carcinoma-associated Endothelial Cells Correlates with Locally Aggressive Primary Tumor Features and Increased Vascular Density

Phyu Aung[1], Edwin Parra[1], Souptik Barua[2], Barbara Mino[1], Jonathan Curry[3], Priyadharsini Nagarajan[3], Carlos Torres-Cabala[1], Alexander Lazar[1], Victor Prieto[1], Ignacio Wistuba[1], Michael Tetzlaff[1]
[1]The University of Texas MD Anderson Cancer Center, Houston, TX, [2]Rice University, Houston, TX, [3]Houston, TX

Disclosures: Phyu Aung: None; Edwin Parra: None; Souptik Barua: None; Barbara Mino: None; Jonathan Curry: None; Priyadharsini Nagarajan: None; Carlos Torres-Cabala: None; Alexander Lazar: None; Victor Prieto: None; Ignacio Wistuba: None; Michael Tetzlaff: None

Background: Merkel cell carcinoma (MCC) is an aggressive cutaneous malignancy whose pathogenesis and prognosis are closely linked with the integrity of the host immune system. Despite promising clinical responses to immune checkpoint blockade (ICB), response and resistance to ICB remain unpredictable, underscoring a critical need to delineate additional prognostic and predictive biomarkers and/or novel therapeutic targets for this disease.

Design: We screened 10 MCCs for expression of immune regulatory markers (PD-L2, B7-H3, B7-H4, IDO-1, ICOS, TIM3, LAG3, VISTA and OX-40) using immunohistochemistry. Among these markers, a subset of MCCs strongly expressed B7-H3 in the endothelial cells restricted to the boundaries of the tumor. Multiplex immunofluorescence (mIF) precisely quantified CD31 and B7-H3 in 52 MCCs. B7-H3 and CD31 expression were tabulated as a series of independent (X,Y) coordinates. A spatial co-localization ratio was estimated using the distribution of distances of B7-H3+ (X,Y) coordinates around the CD31+ (X,Y) coordinates. A spatial G-function calculated within any given radius, what percentage of CD31+ cells overlapped with a B7-H3+ cell.

Results: MCC exhibits a dynamic range of co-localized CD31 and B7-H3 expression. Increasing co-localized expression of B7-H3 with CD31 significantly associated with increased tumor size (p=0.0060), greater depth of invasion (p=0.0110), presence of lymphovascular invasion (p=0.0453) and invasion beyond skin (p=0.0428). Consistent with these findings, increasing co-localized expression of B7-H3 and CD31 correlated with increasing vascular density in MCC.

Conclusions: Our results demonstrate that co-localized expression of B7-H3/CD31 is a poor prognostic indicator and suggest that therapies targeting B7-H3 may represent an effective approach to augmenting immune-activating therapies for MCC.

469 Acral Lentiginous Subtype is an Indicator of Worse Survival in Early Stage (T1) Melanoma

Phyu Aung[1], Denai Milton[1], Doina Ivan[2], Dinesh Pradhan[1], Priyadharsini Nagarajan[2], Michael Tetzlaff[1], Jonathan Curry[2], Victor Prieto[1], Carlos Torres-Cabala[1]
[1]The University of Texas MD Anderson Cancer Center, Houston, TX, [2]Houston, TX

Disclosures: Phyu Aung: None; Denai Milton: None; Doina Ivan: None; Dinesh Pradhan: None; Priyadharsini Nagarajan: None; Michael Tetzlaff: None; Jonathan Curry: None; Victor Prieto: None; Carlos Torres-Cabala: None

Background: Acral-lentiginous melanoma (ALM) is a rare subtype, regarded as more aggressive than other melanomas. To determine whether worse clinical outcome is due to biological behavior or higher stage at presentation, we evaluated a large series of thin (T1) melanomas.

Design: We reviewed the clinicopathological features of 826 T1 melanoma patients (128 [15%] ALM and 698 [85%] non-ALM). We determined associations between clinical and histopathologic parameters, overall (OS) and disease-specific survival (DSS).

Results: 82 (15%) ALM and 453 (85%) non-ALM cases were T1a (Breslow thickness <0.8mm without ulceration) while 46 (16%) ALM and 245 (84%) non-ALM were T1b (Breslow thickness <0.8mm with ulceration or those with Breslow thickness 0.8-1.0mm with/without ulceration). Several statistically significant differences (see table) were found between T1 ALM and non-ALM cases. T1 ALM patients were older (56.1 versus 50.7 years), predominantly females and non-Caucasian; tumors revealed higher frequency of perineural invasion, spindled and nevoid cytology, positive sentinel lymph nodes (SLN), and positive non-SLN. T1 non-ALM tumors showed higher Clark level, frequent regression, brisk tumor-infiltrating lymphocytes, and vertical growth phase. ALM patients experienced higher rates of local recurrence and distant metastases. With median follow-up time was 84.5 months, the 5- and 10-year OS rates for T1 ALM and non-ALM patients were 81% and 67% and 96% and 87%, respectively (p<0.0001). OS was also associated with male gender, older age, and positive SLN status. ALM was not significantly associated with worse OS when adjusting for other measures. The 5- and 10-year DSS rates for T1 ALM and non-AM patients were 90% and 82% and 99% and 98%, respectively (p<0.0001). Regression and positive SLN status were also significantly associated with DSS, with mitotic rate approaching significance. In contrast to OS, ALM subtype was significantly associated with worse DSS when adjusting for other measures (HR=5.3; p=0.025); significance was reached for T1a but not for T1b ALM.

	Histologic Type		
Measure	**ALM** **(N=128)**	**Non-ALM[a]** **(N=698)**	**p-value[b]**
Gender, n (%)			
Male	42 (33)	355 (51)	<0.001
Female	86 (67)	343 (49)	
Age (years)			
Median (range)	56.1 (9.8 – 99.4)	50.7 (2.3 – 87.7)	0.002[c]
Race/ethnicity, n (%)			
Caucasian	95 (78)	677 (97)	<0.0001[d]
Hispanic	18 (15)	15 (2)	
Other	9 (7)	6 (1)	
Clark level, n (%)			
II	57 (45)	174 (25)	<0.0001[d]
III	37 (29)	369 (53)	
IV	34 (27)	153 (22)	
V	0	1 (0.1)	
Perineural invasion, n (%)			
Absent	127 (98)	675 (100)	0.026
Present	2 (2)	0	
Regression, n (%)			
Absent	101 (80)	463 (70)	0.032
Present	26 (20)	200 (30)	
Tumor-infiltrating lymphocytes, n (%)			
Non-brisk/minimal	119 (98)	566 (86)	<0.0001
Brisk	2 (2)	89 (14)	
Vertical growth phase, n (%)			
Absent	60 (50)	116 (18)	<0.0001
Present	61 (50)	538 (82)	
Predominant cytology, n (%)			
Epithelioid	88 (70)	392 (93)	<0.0001[c]
Spindle	9 (7)	18 (4)	
Nevoid	28 (22)	10 (2)	
Sentinel lymph nodes, n (%)			
Negative	64 (83)	670 (96)	<0.0001
Positive	13 (17)	29 (4)	
Non-sentinel lymph nodes, n (%)			
Negative	12 (60)	127 (99)	<0.0001
Positive	8 (40)	1 (1)	
Local recurrence, n (%)			
No	105 (94)	697 (100)	<0.0001
Yes	7 (6)	2 (0.3)	
Distant metastases, n (%)			
No	117 (91)	687 (98)	<0.0001
Yes	12 (9)	12 (2)	

Conclusions: Based on the largest single institutional study of T1 ALM with long follow up, our data reveals that in patients with T1 (and specifically T1a) melanoma, ALM subtype *per se* is associated with a significantly worse DSS. This finding may indicate that ALM is, from its early stages, biologically more aggressive than non-ALM.

470 Clinical Impact of SNP Microarray/FISH Molecular Studies in the Diagnosis of Ambiguous Melanocytic Tumors

Ashley Bradt[1], Paul Harms[1], Lori Lowe[1], Alison Durham[1], Douglas Fullen[1], Rajiv Patel[1], May Chan[1], Min Wang[1], Nicholas Zoumberos[2], Aleodor Andea[1]
[1]University of Michigan, Ann Arbor, MI, [2]Ann Arbor, MI

Disclosures: Ashley Bradt: None; Paul Harms: None; Lori Lowe: None; Alison Durham: None; Douglas Fullen: None; Rajiv Patel: None; May Chan: None; Min Wang: None; Nicholas Zoumberos: None; Aleodor Andea: None

Background: For the great majority of melanocytic tumors, histopathologic examination remains the gold standard for diagnosis. There is, however, a subset of melanocytic lesions that cannot be definitively classified as benign or malignant using histopathological criteria alone. In recent years, molecular methods based on the detection of copy number changes by single nucleotide polymorphism (SNP) microarrays or fluorescence in-situ hybridization (FISH) are increasingly being used as ancillary tests in the diagnosis of histologically ambiguous melanocytic tumors. However, data regarding their use in clinical practice is currently lacking. In this study we evaluated the pattern of use of these tests in clinical practice and the impact that these tests have on changing the final diagnosis for borderline melanocytic tumors.

Design: A total of 126 cases with molecular tests for diagnostics (SNP-array, n=60 or FISH, n=67) were retrieved. Dermatopathology and molecular pathology reports were reviewed and the following information was collected: type of melanocytic lesion, interpretation of the lesion without molecular results and final interpretation incorporating the molecular findings.

Results: A total of 120 cases were diagnosed as borderline before the SNP-array / FISH results. Of these, 12.5%, 53.3% and 32.2% were sub-classified as borderline low risk, borderline intermediate risk, and borderline high risk, respectively. Three cases were diagnosed as melanoma and 3 as atypical nevus; in these, molecular studies were performed for reasons other than risk assessment and thus were excluded from further analysis. The types of lesions for which molecular testing were performed are shown below (Table). Molecular testing was most commonly employed for atypical Spitz tumors and melanocytic tumors of uncertain malignant potential, not otherwise specified (MELTUMP NOS). Out of the 120 borderline lesions, the diagnosis was changed in 96 (80%) to either favoring a low risk / nevus (49 cases) or high risk / melanoma (47 cases). FISH demonstrated a higher failure rate in impacting the diagnosis compared to SNP-array (23% vs 17%, respectively).

Type	No.	Initial risk estimate without molecular results			% with change in diagnosis
		Borderline low risk	Borderline intermediate risk	Borderline high risk	
Spitzoid	42	6	26	10	78.6%
MELTUMP NOS	49	5	18	26	79.6%
BAP1-inactivated tumors	10	1	7	2	100%
Atypical DPN-like tumors	7	1	5	1	71.4%
Atypical cellular blue nevus	4	1	3	0	75%
Other*	8	1	5	2	75%
Total	120	15	64	41	80%

*Other category includes: nevoid melanoma-like tumors (3), congenital nevus lesions (2), atypical halo nevus, pigment synthesizing tumor and subungual junctional melanocytic proliferation (1 each).

Conclusions: Our study demonstrates that use of SNP-microarray / FISH ancillary studies in clinical practice results in a more definitive risk stratification of borderline melanocytic tumors in 80% of cases, with higher success rates for SNP-microarray.

471 Annual Incidence of Melanoma in a City of Vale do Itajaí River from 2001 to 2017 - A Call for Action

Karla Casemiro[1], Beliza Loos[1], Adma Silva de Lima[2], Carolina Fissmer Sardagna[3]
[1]Vitalab Diagnósticos, Brusque, SC, Brazil, [2]Brusque, SC, Brazil, [3]FURB, Blumenau, SC, Brazil

Disclosures: Karla Casemiro: None

Background: Cutaneous melanoma is one of the most lethal cutaneous malignancies and its incidence is increasing worldwide. Australia and New Zealand are considered the countries with the highest melanoma rates in the world. This study was conducted in order to verify the incidence rates in Brusque - Santa Catarina, a city in the south of Brazil and compare its incidence with cities nearby and around the globe.

Design: A search was conducted on the sole pathology laboratory of the city and the number of melanoma cases diagnosed from 2001 to 2017 was computed, as long as some clinical and epidemiological data. These data were then compared with the estimated population of the city, according to Brazilian Institute of Geography and Statistics (IBGE) for the period.

Results: Incidence rates rose from 6,4 cases/100.000 inhabitants in 2001 to 61,3 cases/100.000 inhabitants in 2017, demonstrating a 10-fold increase in the period. In some years, there was a statistically significant female prevalence. Although an increase number of technologies and devices have emerged on the last decades to aid in early diagnosis, many cases area already invasive when diagnosed.

Tabela 1 – Incidência de melanoma in situ e invasivo. 2001 a 2017.

Year	Estimated Population	Number of cases			Incidence(per 100.000 population)			Statistic z	P
		in situ	invasive	in situ + invasive	in situ	invasive	in situ + invasivo		
2001	78152	1	4	5	1,28	5,12	6,40	1,34	0,1797
2002	79815	4	7	11	5,01	8,77	13,78	0,90	0,3657
2003	81558	5	5	10	6,13	6,13	12,26	0,00	1,0000
2004	85218	3	9	12	3,52	10,56	14,08	1,73	0,0833
2005	87244	4	6	10	4,58	6,88	11,46	0,63	0,5271
2006	89254	4	10	14	4,48	11,20	15,69	1,60	0,1088
2007	95453,9	5	4	9	5,24	4,19	9,43	0,33	0,7389
2008	99917	10	8	18	10,01	8,01	18,01	0,47	0,6373
2009	102280	8	14	22	7,82	13,69	21,51	1,28	0,2008
2010	105431	15	8	23	14,23	7,59	21,82	1,46	0,1444
2011	107763	9	16	25	8,35	14,85	23,20	1,40	0,1615
2012	109950	35	18	53	**31,83**	**16,37**	48,20	2,34	**0,0195**
2013	116634	26	12	38	**22,29**	**10,29**	32,58	2,27	**0,0231**
2014	119719	23	19	42	19,21	15,87	35,08	0,62	0,5371
2015	122775	23	20	43	18,73	16,29	35,02	0,46	0,6473
2016	125810	31	17	48	**24,64**	**13,51**	38,15	2,02	**0,0433**
2017	128818	41	38	79	31,83	29,50	61,33	0,34	0,7357

I – P: Value-P of the Independent Proportion Test. If P <0.05 then significant differences between incidences.

Figure 1 - 471

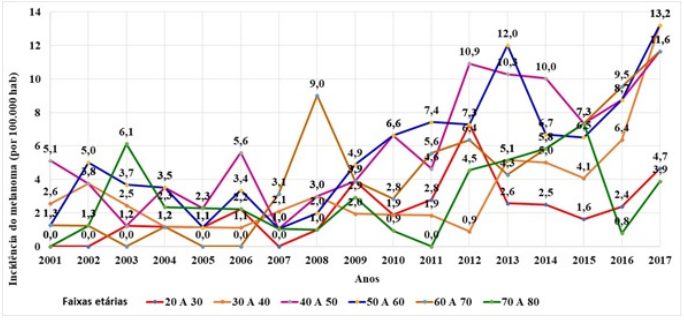

Figure 1 - Incidence of melanoma according to age group. 2001 to 2017.

Figure 2 - 471

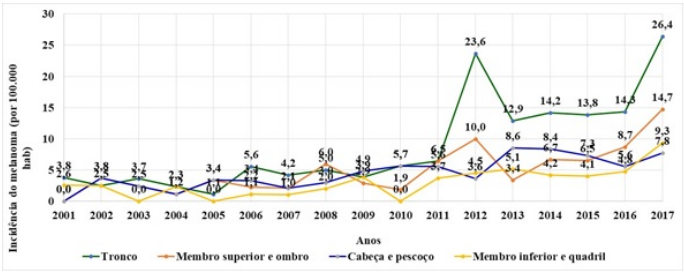

Figure 2 - Incidence of melanoma according to location. 2001 to 2017.

Conclusions: Melanoma incidence is high and increasing in the city, reaching proportions similar to Australia. These data are in accordance to previous reported data from cities nearby. There is an urgent need to address these high incidences of the disease, due to its importance and costs involved.

472 Treponema Pallidum Immunohistochemical Detection of Syphilis in Biopsies: One Institution Experience

Muhan Joyce Chen[1], Garrett Desman[1]
[1]*Icahn School of Medicine at Mount Sinai, New York, NY*

Disclosures: Muhan Joyce Chen: None

Background: There has been a recent rise in reported cases of syphilis in the HIV-positive and men who have sex with men (MSM) populations within New York City. Primary ulcers (chancre) may arise in anogenital sites and the oral mucosa. Secondary syphilis is characterized by a widespread erythematous maculopapular eruption, often involving the palms and soles. Despite these classic clinical features, atypical presentations are common; therefore, it is crucial for the pathologist to maintain a high index of suspicion for this disease. In addition to serological studies (i.e. rapid plasma reagin [RPR]) a Treponema immunohistochemical stain (IHC) has recently become available. Herein, we summarize our clinicopathologic experience with syphilis and its detection using IHC and RPR.

Design: A natural language search of our pathology records at the Mount Sinai Hospital (2013-2018) for “syphilis” yielded 38 patients with a diagnosis confirmed by clinicopathologic correlation. Only 15 cases were annotated with both RPR and TreponemaIHC staining information. A review of the H&E and IHC slides (Treponema Pallidum antibody, Biocare Medical), as well as the clinical and serological findings was performed.

Results: Of the 15 cases in our cohort, 53.3% consisted of anal/genital biopsies, 33.3% were skin biopsies other than genitalia, and 13.3 % were miscellaneous biopsies. Patients included 1 female and 14 males with an average age of 40 years (range: 27–68 years). All patients included 6 whites (40%), 1 Asian-American (6%), 4 Hispanic-Americans (27%) and 4 Africa-Americans (27%). Four patients were human immunodeficiency virus (HIV) positive, and 2 patients were partnered with HIV positive partners. The most common presenting symptoms were “skin rash” (n=6, 40%), “penile ulcer” (n=3, 20%), and “anal ulcer/mass” (n=5, 33%) and “lip ulcer” (n=1, 7%). Treponema IHC staining revealed a sensitivity of 50% and a specificity of 89% for diagnosing primary and secondary syphilis. RPR titers in 3 of 15 cases fell below the designated threshold and were considered negative. The resulting RPR serological studies revealed a sensitivity of 62.5% and specificity of 86% in our cohort. The 3 cases with negative Treponema IHC and high RPR titers were recently treated with penicillin at the time of biopsy. This finding may be important in the proper interpretation of IHC staining.

Conclusions: Our experience suggests that the Treponema IHC stain has limited sensitivity when used alone without serological studies and clinicopathologic

473 SOX10-Positive Perivascular Cells in Sentinel Lymph Nodes: A Reliable Internal Control

Lorraine Colon Cartagena[1], Steven Smith[2], Mark Mochel[2]
[1]*Virginia Commonwealth University, Richmond, VA,* [2]*Virginia Commonwealth University School of Medicine, Richmond, VA*

Disclosures: Lorraine Colon Cartagena: None; Steven Smith: None; Mark Mochel: None

Background: Sentinel lymph node (SLN) positivity for metastatic melanoma strongly correlates with poor prognosis and has major implications for adjuvant therapy. Immunohistochemistry (IHC) for melanocytic markers is used routinely to assist in SLN examination for subtle involvement, and recent studies have demonstrated SOX10 to be a sensitive and specific marker with advantageous sharp nuclear staining. Given that IHC relies on positive controls to ensure true negativity for metastasis, internal tissue controls possess great value. To the authors' knowledge, a rigorous examination of SOX10 IHC on SLNs for prevalence of internal controls has not been reported, and is distinctly salient in light of ongoing recalls of IHC systems and reagents.

Design: A retrospective, consecutive series of SLNs reviewed and identified as negative for melanoma by routine H&E and IHC for SOX10 were reviewed. IHC for SOX10 was evaluated for the presence of internal tissue positive controls, including nerves, nodal nevus, and other cells.

Results: From a total of 42 patients, negative SLNs, previously examined by SOX10 immunohistochemistry, were reviewed. This included 109 IHC slides for SOX10. Of these, 107 (98%) demonstrated at least one internal positive control. Positive-staining nerves were present in 67 cases (61%), while incidental capsular melanocytic nevi were seen in 8 cases (7%). Of note, scattered, small SOX10+ spindle cells were seen in a perivascular distribution in 107 cases (98%). On adjacent H&E stained sections, these perivascular cells corresponded to spindle cells with scant cytoplasm and small elongated nuclei.

Conclusions: In addition to the previously reported advantages of SOX10 IHC in sensitivity, specificity, and subcellular staining pattern for melanoma detection in SLNs, IHC for SOX10 demonstrates consistent positivity for readily identifiable internal positive controls, including the novel finding of perivascular SOX10-positive spindle cells, the latter apparent in approaching 100% of cases. The nature of these perivascular SOX10-positive cells is not presently well-characterized biologically or histogenetically. However, these cells are reliably present in SLN sections and provide a pervasive internal positive control for technical fidelity in one of the most fraught diagnostic scenarios in all of surgical pathology.

474 The Role of Human Commensal Skin Bacteria in the Pathogenesis of Cutaneous T Cell Lymphoma

Carina Dehner[1], William Ruff[2], Thaddeus Stappenbeck[1], Martin Kriegel[2]
[1]*Washington University School of Medicine, St. Louis, MO,* [2]*Yale University School of Medicine, New Haven, CT*

Disclosures: Carina Dehner: None; William Ruff: None; Thaddeus Stappenbeck: None; Martin Kriegel: *Employee*, Roche; *Primary Investigator*, Patent from Yale

Background: Cutaneous T cell lymphoma (CTCL) is a malignancy of transformed skin-homing T cells. CTCL is thought to arise from a combination of genetic, epigenetic and environmental factors, but the stimuli that trigger and sustain T cell proliferation in skin lesions remain unclear. We investigated if adaptive immune responses to skin commensals within CTCL lesions induce clonal T cell proliferation in genetically predisposed patients

Design: We sampled blood, stool and lesional vs non-lesional skin of 10 CTCL patients longitudinally at up to four time points. Samples from SLE patients and healthy donors were collected to serve as controls. Dual-index V1-3 and V4 16S rRNA sequencing was performed on the Illumina MiSeq platform. Resident aerobic bacteria was cultured from lesional and adjacent non-lesional skin of five CTCL patients. In addition, malignant cutaneous T cells were isolated from patient biopsies for testing STAT3 phosphorylation ex vivo and commensal-induced T cell proliferation in vitro. A FISH probe for *B. safensis* was used to stain lesional biopsies from a selected subset of CTCL and control (psoriasis) patients

Results: 16S rRNA profiling showed dysbiosis in CTCL skin compared to controls. Culturing of skin lesions revealed unique bacterial strains compared to adjacent non-lesional sites. The most consistent isolate for lesional CTCL skin was *Bacillus safensis*, a Gram-positive, spore-forming rod. Next, lesional T cells were isolated to demonstrate increased STAT3 phosphorylation in lesional vs non-lesional skin, supporting features of CTCL cells besides routine TCR phenotyping. Co-cultures with patient-isolated skin symbionts showed that T cells from 3 CTCL patients significantly proliferated in response bacterial populations from lesionally enriched bacteria as compared to non-lesional bacteria. Phenotypic profiling of these cells after stimulation with *B. safensis* supported a pro-inflammatory state with increased IL-17A, IFN-γ and IL-21. FISH confirmed *B. safensis* preferentially localized to CTCL skin lesions as compared to psoriasis lesions.

Conclusions: The results of our project studying cancer cell-microbiota interactions suggest skin commensal candidates being involved in the pathogenesis of CTCL. Pathobionts enriched in lesional skin might act as antigenic stimulus leading to clonal transformation of cutaneous T cells, similar to the pathogenesis of *H. pylori*-induced MALT lymphoma, a paradigm that may be applicable to skin lymphomagenesis

475 Targeted Genomic Profiling of Melanoma of Unknown Primary Site Reveals Mutational Profile Similar to Cutaneous Melanoma

Mia DeSimone[1], Navin Mahadevan[1], Phani Davineni[1], George Murphy[2], Christine Lian[1], Fei Dong[1]
[1]Brigham and Women's Hospital, Boston, MA, [2]Harvard University, Boston, MA

Disclosures: Mia DeSimone: None; Navin Mahadevan: None; Phani Davineni: None; George Murphy: None; Christine Lian: None; Fei Dong: None

Background: Melanoma of unknown primary site (MUP) may represent metastasis from a clinically covert primary melanoma or cutaneous melanoma with regression of the primary site. Cutaneous and mucosal melanomas demonstrate significant genomic differences in oncogenic mutations, ultraviolet radiation-associated (UVR) mutagenesis, and burden of total somatic mutations. This study evaluates molecular characteristics of MUP and assesses whether they most likely arise from a cutaneous origin to inform therapeutic approaches and prognostication.

Design: Malignant melanoma cases (n=121; 90 cutaneous, 20 MUP, 10 mucosal, and 1 ocular) were genotyped using a targeted next-generation sequencing assay of 275 oncogenes and tumor suppressor genes. Tumors were classified based on the Cancer Genome Atlas subtypes according to the presence of *BRAF*, *NRAS,* and *NF1* mutations. Total mutational burden and the presence of UVR mutational signature were assessed.

Results: *BRAF* activating mutations were identified in 36% (n=32/90) of cutaneous melanomas, 25% (5/20) of MUP, and 9% (1/11) of mucosal and ocular melanomas. *NRAS* activating mutations were identified in 33% (30/90) of cutaneous melanomas, 30% (6/20) of MUP, and 18% (2/11) of mucosal and ocular melanomas. Triple wild-type, or lack of hot-spot *BRAF*, *N/H/K-RAS*, or *NF1* mutations, constituted 21% (19/90) of cutaneous melanomas, 20% (4/20) of MUP, and 64% (7/11) of mucosal and ocular melanomas. UVR mutational signature, defined by enrichment of C>T transitions in dipyrimidine sites, was seen in most MUP (85%, 17/20) and cutaneous melanomas (74%, 67/90) and no mucosal or ocular melanomas (0/11). Melanomas with UVR signature exhibited higher total mutational burden (median 21.1 per Mb) than melanomas without UVR signature (median 8.4 per Mb). The total mutational burden of MUP (median 16.8 per Mb) was similar to that of cutaneous melanomas (median 18.0 per Mb), compared to a lower total mutational burden in mucosal and ocular melanomas (median 8.4 per Mb).

Conclusions: MUP display a mutational profile comparable to cutaneous melanomas, including frequent mutations in *BRAF* and *NRAS*, UVR mutational signature, and high total mutational burden. These findings support MUP as metastatic melanomas from sun-exposed cutaneous primary sites and inform clinical approaches to detection of covert or regressed primary sites. Moreover, patients with MUP may benefit from systemic therapy proven effective for UV-induced melanomas, including *BRAF* inhibition and immune checkpoint blockade.

476 Contribution of Deep Neural Network to the Diagnosis of Spitz Tumors

Christine Devalland[1], Nabil Omri[2], Karima Mrad[3], Ryad Zemouri[4], Mounir Sayadi[5], Noureddine Zerhouni[6]
[1]Hopital Nord Franche Comte France, Belfort, France, [2]FEMTO-ST, Besancon, France, [3]Institut Salah Azaiez, Tunis, Tunisia, [4]Cnam, Paris, France, [5]ENSIT, Tunis, Tunisia, [6]ENSMM, Besancon, France

Disclosures: Christine Devalland: None; Nabil Omri: None; Karima Mrad: None ; Ryad Zemouri: None; Noureddine Zerhouni: None

Background: Spitz tumors (ST) are rare melanocytic tumors classified in Spitz Nevi (SN) and Atypical Spitz Tumor (AST). This classification is based on histological features and immuno-markers .Deep Learning Neural Networks (DLNN) is an artificial intelligence (Ai).This work is about the potential contribution of AI in Spitz tumors diagnosis and analyze the link between histological profiles and immune markers (IM) in spitz tumors.

Design: A DLNN is composed of “neurons” distributed over different layers. Each neuron of a layer is connected to all the neurons of the next layer through a weighted arc. The DLNN training consists in computing the weights of the arcs, using a training data set composed of the input values and the expected ouput values. Then, the DLNN can interpolate any result from any unknown input value. We analysed 53 ST (47 NS and 6 TSA) with 10 clinical datas , 11 histological datas (diameter, thickness ,mitosis count , cytonuclear atypia, subcutis extension, asymmetry, poor circumscription, pagetoid spread, lymphocytic infiltrate, high cellular density and Kamino bodies) and 6 IM (Melan-A, HMB-45, P16 ,KI 67 ,BRAFV600E and ALK).We have trained and tested DLNN for 4 tests composed of 27 inputs and one out put : Diagnosis ; BRAF status; ALK status ;BRAF and ALK status. For these different scenarios, the k-cross validation (k=3) has been used. The main idea of this method is to divide the data set into k sub-sets and to use (k-1) subsets for the training phase and the remaining subset to the test phase.

Results: DLNN trained on tumors classified correctly 87% of NS and only 50% of ATS. None immunomarker was recognize as specific by DLNN. Braff status is evaluated correctly at 84 %, and Alk status at 85 %. For BRAFF and ALK status there is no specifically histological profile by DLNN.

Table 1: Summary of the simulations results.

	Scenario 1	Scenario 2	Scenario 3	Scenario 4
Accuracy	91.67 % ± 3.61 %	85.42 % ± 7.22 %	93.75 % ± 6.25 %	77.08 % ± 3.61 %

Conclusions: This study concerns the use of DLNN in the classification of Spitz tumors. It does not allow on this limited cohort to definitively distinguish SN from AST.These preliminary results are encouraging and may be pursued by a larger cohort study to determine the relevance and preponderance of an immune-marker.

477 DNA Mismatch Repair Deficient Keratoacanthomas are Histologically Indistinguishable from MMR Proficient Ones and Do Not Show MLH1 Promoter Methylation

Renee Eigsti[1], Brian Swick[2], Rondell Graham[3], Andrew Bellizzi[2]
[1]Iowa City, IA, [2]University of Iowa Hospitals and Clinics, Iowa City, IA, [3]Mayo Clinic, Rochester, MN

Disclosures: Renee Eigsti: None; Brian Swick: None; Rondell Graham: None; Andrew Bellizzi: None

Background: Keratoacanthoma (KA), a peculiar, spontaneously regressing squamous tumor, is seen in the Muir-Torre variant of Lynch syndrome. We previously identified 48 DNA mismatch repair deficient (dMMR) KAs in 46 patients among an institutional cohort of 1353 KAs in 1067 patients (4.3% of patients; *Mod Pathol*. 2016;29(Suppl 2):127A). In colon cancer, dMMR tumors have characteristic histologic features compared to MMR proficient (pMMR) ones. MLH1-deficiency (MLH1d) predominated in our dMMR KAs (74%). In other tumor types characterized by frequent dMMR (e.g., colon, endometrium), among MLH1d tumors, sporadic tumors due to *MLH1* promoter methylation outnumber Lynch-associated ones on the order of 5-10:1. We sought to compare the histologic features of dMMR KAs with age and gender matched controls and to identify any sporadic dMMR tumors.

Design: Each dMMR KA (34 MLH1d, 12 MSH2d, 2 MSH6d) was age and gender matched to 2 pMMR controls. Original glass slides of these 144 tumors were blindly reviewed for the presence of tumor infiltrating lymphocytes, peritumoral lymphocytes, and lymphoid aggregates in the adjacent stroma. The frequency of these features was compared in cases and controls, using two-tail Fisher's exact tests ($p<0.05$ considered significant). *MLH1* promoter methylation testing was attempted on 20 MLH1d KAs with the most abundant residual tumor tissue.

Results: The 48 dMMR KAs occurred in 32M:16W, ages 41-92 years (mean 75; median 76); the 96 pMMR KAs occurred in 63M:33W, ages 41-92 years (mean 75; median 76). The frequency of tumor infiltrating lymphocytes, peritumoral lymphocytes (both common), and lymphoid aggregates (less common) was similar in cases and controls (see Table). All 9 tumors in which *MLH1* promoter methylation testing was successful were unmethylated; testing failed in 11 tumors. Testing was performed twice on each of the 20 tumors, with all results concordant.

Histologic Feature	Frequency in Cases (dMMR)	Frequency in Controls (pMMR)	p
Tumor infiltrating lymphocytes	90% (43/48)	84% (81/96)	0.45
Peritumoral lymphocytes	88% (42/48)	89% (85/96)	1
Lymphoid aggregates	17% (8/48)	14% (13/96)	0.62

Conclusions: 4% of KAs are dMMR. Unlike other dMMR tumors, they are histologically similar to their pMMR counterparts. This likely reflects the prominent role of the tumor-associated lymphoid response in the spontaneous regression of all KAs. *MLH1* promoter methylation does not appear to play a role in the formation of sporadic MLH1d KAs. We are currently performing biallelic *MLH1* mutation testing to rule out this less common mechanism of sporadic dMMR tumor formation.

478 Potential Utility of GATA3 as a Predictive Biomarker for Disease Progression in Mycosis Fungoides

Gerard Frigola[1], Andrea Combalia[1], Teresa Estrach[1], Adriana Garcia Herrera[2]
[1]Hospital Clinic of Barcelona, Barcelona, Spain, [2]Hospital Clinic, Barcelona, Spain

Disclosures: Gerard Frigola: None; Andrea Combalia: None; Teresa Estrach: None; Adriana Garcia Herrera: None

Background: Large cell transformation (LCT) in mycosis fungoides (MF), defined as having more than 25% of infiltrating atypical T-cells or clusters of large cells, has been reported to have a more aggressive disease course with shortened overall survival compared with MF without LCT. In addition, it has been described that neoplastic T-cells in early MF show a predominant T_H1 phenotype with T-bet expression, and that progression to tumor stage is associated to a T_H2 phenotype shift with expression of GATA3. Nevertheless, it has been shown that GATA3 expression can be already found in up to one third of early stage MF. Our aim is to assess the validity of GATA3 and T-bet expression as prognostic biomarkers for disease progression.

Design: We reviewed 46 samples obtained longitudinally from 11 patients with MF during the period 1995-2018 and collected relevant clinical information for each case. Disease progression was defined as increase in clinical stage or death due to MF. Immunophenotypic characterization of tumoral cells included T-cell markers CD2, CD3, CD5, CD7, CD4, CD8 and CD30, as well as T-cell subset markers GATA3 and T-bet. T-cell subset markers were evaluated in neoplastic cells, recognized by their location and morphology. A cutoff of >10% of GATA3 positive neoplastic T-cells was used to establish GATA3+ phenotype.

Results: GATA3+ phenotype was observed in all cases with disease progression (6/6). Moreover, GATA3 expression was seen in 100% (8/8) of cases displaying LCT: 25% of patients displayed LCT with GATA3+ phenotype at the time of initial diagnosis of MF; 25% of the cases exhibited GATA3 expression in LCT biopsies from patients previously diagnosed of MF; and 50% of patients showed expression of GATA3 in follow-up biopsies of plaque stage lesions before their histological transformation. Three cases were negative for GATA3 and didn't show either clinical progression or LCT in the sequential biopsies. T-bet expression was rather stochastic and was not associated with disease progression nor histological transformation

Conclusions: GATA3 expression seems to be a good prognostic marker of large cell transformation in MF, appearing in 50% of cases of our series before the transformation. With this preliminary result, we will assess GATA3 expression in a series of 120 cases of MF with >5 years of follow-up in order to study the potential value of GATA3 as a predictive marker of disease progression in MF. Results will be provided by the time of the congress.

479 INSM1 Immunohistochemical Evaluation of Merkel Cell Carcinoma and Other Cutaneous Epithelial Tumors

Joseph Frye[1], Richard Mertens[2], David Frishberg[3], Bonnie Balzer[1], Wonwoo Shon[4]
[1]Cedars-Sinai Medical Center, Los Angeles, CA, [2]Sherman Oaks, CA, [3]Cedars-Sinai Medical Center, West Hollywood, CA, [4]Cedars-Sinai Medical Center, Studio City, CA

Disclosures: Joseph Frye: None; Richard Mertens: None; David Frishberg: None; Bonnie Balzer: None; Wonwoo Shon: None

Background: INSM1, a zinc-finger transcription factor, has emerged as a robust diagnostic marker of neuroendocrine differentiation. Recent studies have shown that it is also a sensitive marker for Merkel cell carcinoma (MCC). However, INSM1 expression has not been systematically examined in other cutaneous epithelial tumors and studies have been limited regarding the relationship of INSM expression to Merkel cell polyomavirus (MCPyV) status. In this study, we analyzed a large number of well-characterized MCC and other cutaneous epithelial tumors for INSM1 expression. Presence of MCPyV was also investigated.

Design: Formalin-fixed, paraffin-embedded whole and tissue microarray sections from 63 MCC and 147 cutaneous epithelial tumors (104 adnexal tumors, 24 squamous cell carcinomas, 14 basal cell carcinomas, and 5 clear cell acanthomas) were obtained and immunostained for INSM1 (clone A8, Santa Cruz Biotechnology). In addition, all MCC cases were also stained with CM2B4 to measure MCPyV large T-antigen expression.

Results: INSM1 nuclear positivity was seen in 55/63 (87%) MCC (41/43 MCPyV-positive and 14/20 MCPyV-negative). All the other tumor types were completely negative for INSM1 expression, apart from follicular adnexal tumors with colonizing Merkel cells (6 trichofolliculomas, 4 trichilemmomas, and 2 desmoplastic trichoepitheliomas). In 2 cases of pilomatricoma, rare osteoclast-like giant cells were also positive for INSM1.

Conclusions: The sensitivity and specificity of INSM1 with regards to the cases evaluated in this study are comparable or better than that of established diagnostic neuroendocrine markers. No significant association was apparent between INSM1 expression and MCPyV status. Finally, INSM1-positive non-neoplastic Merkel cells were frequently associated with tumors with follicular differentiation.

480 Morphological and Molecular Characteristics of Skin Tumors in Hepatocellular Carcinoma Patients under Sorafenib Treatment

Carla Fuster[1], Leonardo Da Fonseca[1], Victor Sapena[1], Álvaro Díaz-González[1], Loreto Boix[1], Marco Sanduzzi-Zamparelli[1], Esther Samper[1], Neus Llarch[1], Gemma Iserte[1], Ferran Torres[1], Manel Solé[1], Jordi Bruix[1], Maria Reig[1], Alba Diaz[1]
[1]Hospital Clinic of Barcelona, Barcelona, Spain

Disclosures: Carla Fuster: None; Leonardo Da Fonseca: None; Victor Sapena: None; Álvaro Díaz-González: *Speaker*, Bayer; Loreto Boix: None; Marco Sanduzzi-Zamparelli: None; Esther Samper: None; Neus Llarch: None; Gemma Iserte: None; Ferran Torres: None Manel Solé: None; Jordi Bruix: *Consultant*, Arqule, Bayer, Shering Pharma, Novartis, BMS, BTG-Biocompatibles, Eisai, Kowa, Terumo, Gilead, Bio-Alliance, Roche, AbbVie, Merck, Roche, Sirtex, Ipsen, Astra-medimmune, Incyte, Quirem, Lilly; *Grant or Research Support*, Bayer, BTG; *Speaker*, Bayer, BTG, Ipsen; Maria Reig: *Grant or Research Support*, Bayer, BMS, Ipsen,AstraZeneca, Lilly; Alba Diaz: None

Background: Sorafenib is the first-line systemic therapy for hepatocellular carcinoma (HCC) patients. Early skin reactions are frequent adverse events (mainly rash and hand-foot reaction), which have been correlated with better survival. Few cases of skin tumors in this setting have also been reported. The biological mechanism behind their appearance is unknown, but sorafenib could induce a paradoxical activation of the MAPK pathway in cells without *BRAF* mutations, making them to proliferate. The aim of the study was to describe the pathological and molecular features of a series of skin tumors developed in HCC patients treated with sorafenib.

Design: From March/2008 to November/2017, 313 patients were treated with sorafenib in the BCLC group (Hospital Clínic of Barcelona). Fifteen patients (4,8%) developed one or more skin tumors. Clinical and pathological features were reviewed. Competitive allele-specific taqman PCR (CAST-PCR) for *HRAS (G12D, Q61K, Q61L)*, *BRAF (V600E)* and *KRAS (G12D)* mutations was performed, including a control group.

Results: A total of 21 excised lesions were diagnosed as follows: 6 keratoacanthomas (KA), 5 seborrheic keratosis (SK), 5 basocellular carcinomas (BCC), 4 infiltrating squamous cell carcinomas (SCC) and 1 sebaceous hyperplasia. The most frequent location was head and neck, and limbs. The median time between sorafenib-initiation and the appearance of the first skin tumor was 9 months [IQR; 4.4 to 18.1] and the median OS was 26.5 months (95%CI; 17.03, 43.95). CAST-PCR was performed from 17 available formalin-fixed paraffin-embedded samples. Mutations of *KRAS* and *HRAS* were identified in 5 out of 17 (29,4%) cases while BRAF mutations were not detected. *HRAS* mutations were present in 3 cases (1 SCC, 1 SK and 1 BCC); *KRAS* mutations were detected in the remaining 2 (1 BCC and sebaceous hyperplasia).

Conclusions: This is the largest series describing the morpho-molecular features of skin tumors from HCC patients under sorafenib. As other *RAF* inhibitors, sorafenib seems to induce a spectrum of skin tumors, ranging from benign to malignant but without negative impact on survival. Activating *HRAS* or *KRAS* mutations may play a role in their development. This is the rational to consider skin tumors as a reflection of sorafenib mechanism of action. In addition, the outcome of these patients is quite favorable. Thus, development of skin lesions under sorafenib should become a relevant parameter to consider in the evaluation of second line therapies both in practice and research.

481 Defining the Impact of PD-1/PD-L1 Axis Expression in Melanoma Using Multiplex Immunofluorescence Paired with Flow Cytometry Quantification

Nicolas Giraldo-Castillo[1], Sneha Berry[1], Peter Nguyen[1], Abha Soni[1], Farah Succaria[1], Haiying Xu[1], Ludamila Danilova[1], Alexander Baras[2], Janis Taube[3]
[1]Johns Hopkins Medical Institutions, Baltimore, MD, [2]Baltimore, MD, [3]Johns Hopkins University School of Medicine, Baltimore, MD

Disclosures: Nicolas Giraldo-Castillo: None; Sneha Berry: None; Peter Nguyen: None; Abha Soni: None; Farah Succaria: None; Haiying Xu: None; Ludamila Danilova: None; Alexander Baras: None; Janis Taube: *Advisory Board Member*, Bristol Myers Squibb; *Consultant*, Merck; *Advisory Board Member*, Astra Zeneca; *Grant or Research Support*, Bristol Myers Squibb; *Advisory Board Member*, Amgen

Background: Multiplex IF (mIF) can provide a more detailed characterization of spatial relationships and complex cell phenotypes in the tumor microenvironment (TME) than single-stain chromogenic IHC. However, the data-analysis and visualization mIF can be time-consuming. Here, we capitalized on efficient, established flow cytometry workflows and paradigms to analyze mIF-stained melanoma slides. PD-1 and PD-L1 expression was defined by cell type and then the impact on prognosis of the spatial relationships of these phenotypes within the TME was assessed.

Design: Tissue microarrays composed of 87 primary and metastatic melanoma specimens were stained by mIF for CD8, CD163, FoxP3, PD-1, PD-L1, and melanocyte cocktail (Sox10 and S100). After digital scanning and unmixing (Vectra 3.0), the cell-by-cell data was imported and gated in FlowJo. Median fluorescence intensity was used to determine relative expression across cell lineages. Cell densities and distances between cell types were calculated in R.

Results: Co-expression studies showed that 70% of PD-1+ cells were CD8+ cells. Additionally, PD-1 expression intensity was higher for CD8+ cells than other cell types e.g., FoxP3+PD-1+ cells. Approximately 3x the number of tumor cells expressed PD-L1 compared to CD163+ macrophages, however, macrophages displayed higher intensity PD-L1. Notably, PD-L1 expression intensity was increased when tumor cells or macrophages approximated CD8+ T cells, supporting an adaptive mechanism of expression. When these features were correlated with patient outcomes, increasing CD163+ cell density associated with shorter overall survival (OS, $p<0.001$), while increasing CD8+, PD-1+, and PD-L1+ cell densities correlated with longer OS ($p=0.001$, 0.003, and 0.08, respectively). In particular, high densities of CD8+PD-1+ cells within 20um of a tumor cell strongly associated with favorable OS.

Conclusions: We demonstrate the use of flow cytometry quantification methods to analyze mIF stains on FFPE slides. Our data validate simple prognostic biomarkers (e.g., CD8+ infiltration) previously identified by single-stain IHC. Furthermore, we are able to characterize the intensity of PD-1 and PD-L1 expression by cell type, which has not previously been reported in FFPE samples. This approach also supported studies of co-expression, such that phenotypic sub-populations and their proximities within the TME could be assessed. Such efficient multiparametric approaches will facilitate identification of more robust prognostic biomarkers.

482 Prediction of Prognostic Outcomes in Melanoma Using Digital Cell Count Estimation of Sentinel Lymph Node Tumor Burden

Emily Hartsough[1], Daniel Miller[2], Evidio Domingo-Musibay[2], Alessio Giubellino[2]
[1]University of Minnesota Medical Center, Minneapolis, MN, [2]University of Minnesota, Minneapolis, MN

Disclosures: Emily Hartsough: None; Daniel Miller: None; Evidio Domingo-Musibay: None; Alessio Giubellino: None

Background: Melanoma often metastasizes *in primis* to sentinel lymph nodes (SLN). Currently, there is no numerical threshold of metastatic burden to classify a SLN as positive and the prognostic significance of isolated tumor cells is uncertain. Different criteria have been used to more accurately characterize SLN micrometastatic burden, including Dewar, Rotterdam, and Starz classifications. However, none of these consider the number of cells identified within the sample. Here, we describe a method to classify SLN metastatic burden by using software analysis to count the number of tumor cells within the largest metastatic focus.

Design: Patients with positive SLN biopsies were identified by querying our archival tissue database at the University of Minnesota from 2002-2011. The positive SLN biopsies were reviewed by a board-certified dermatopathologist to confirm the diagnosis among available cases. Histopathologic characteristics and clinical information were collected and used in our analysis. Digital images of the SLN were obtained for software analysis. Patients were separated into groups based on cell count, as outlined in the results section.

Results: We identified 110 cases of SLN biopsies, including 38 that were positive for metastatic melanoma (34.5%). Twenty-four cases were available for final review. Precise cell counting was performed within the greatest metastatic focus. The Fisher exact test was used to compare prognostic factors between groups of patients with <500 cells (n=10), 500-5000 cells (n=6), and >5000 cells (n=8) in their SLN metastasis. On comparison of these three groups, there was a statistically significant difference ($p<0.05$) between cell count within the SLN and development of subsequent metastatic disease ($p=0.0154$). There also was an association observed when comparing cell count to lymph node basin site ($p=0.0273$), morphology of the metastatic focus ($p=0.0004$), maximum diameter ($p=0.0005$), and tumor penetrative depth ($p=0.0036$) of the largest metastatic focus.

Conclusions: These preliminary data support the use of computerized cell count analysis for predicting prognostic outcomes in patients undergoing SLN biopsy. Specifically, there is an association between cell count of the largest metastatic focus in the SLN and subsequent metastatic disease, lymph node basin location, morphology of the metastatic focus, and Rotterdam and Starz criteria. However, follow-up studies are needed in order to increase our population size and confirm these results.

483 Immunohistochemistry in the Distinction of Sebaceous Carcinoma from Squamous and Basal Cell Carcinoma

Christina Hodgson[1], Andrew Bellizzi[1]
[1]University of Iowa Hospitals and Clinics, Iowa City, IA

Disclosures: Christina Hodgson: None; Andrew Bellizzi: None

Background: The distinction of sebaceous (SEBC) from squamous (SCC) and basal cell carcinoma (BCC) can be diagnostically challenging and is clinically important. SEBC is more clinically aggressive, including a propensity for distant metastasis, and, although more common with sebaceous adenoma, it may indicate Lynch syndrome. We read with great interest a recent report that claimed a particular factor XIIIa clone (AC-1A1) showed apparent immunohistochemical (IHC) cross reactivity with an antigen in the nucleus of sebocytes and was a sensitive and specific SEBC marker (PMID: 27153339). This result has been corroborated by another group (PMID: 28873247). We had previously brought up androgen receptor (AR) IHC for SEBC, but results have been disappointing clinically. Ber-EP4 is an established BCC marker in the differential with SCC, but experience in SEBC is more limited.

Design: We performed factor XIIIa (AC-1A1), AR, and Ber-EP4 IHC on tissue microarrays (tumors arrayed as triplicate 1 mm cores) of 21 SEBCs, 15 SCCs, and 42 BCCs. For each marker, intensity (0-3+) and extent (0-100%) of expression were assessed, and an H-score was calculated (intensity*extent). Fisher's exact and Mann-Whitney tests were performed with $p<0.05$ considered significant.

Results: In optimizing AC-1A1 IHC, we observed strong nuclear staining in sebocytes, but we also also observed weaker staining in adjacent squamous epithelium (Figure 1). Not surprisingly, we thus observed similar rates and intensities of AC-1A1 positivity in SEBC (76%; median H-score 42) and SCC (73%; median H-score 60); notably BCCs were uniformly negative. As was our clinical experience, AR was frequently positive in SEBC (81%) but not strongly so (median H-score 57), and often only in the most differentiated areas; BCCs were also often positive (62%), typically with rather intense staining of limited extent (median H-score 13); SCCs were uniformly negative. Ber-EP4 was diffusely, strongly positive (median H-score 255) in 98% of BCCs, but SEBCs were also often strongly positive (72%; median H-score 180); SCCs were again uniformly negative. These results are summarized in the Table.

	Factor XIIIa % Positive	Factor XIIIa Mean (Median) H-score (if positive)	AR % Positive	AR Mean (Median) H-score (if positive)	Ber-EP4 % Positive	Ber-EP4 Mean (Median) H-score (if positive)
Sebaceous carcinoma	76%[1]	59 (42)[2]	81%[3]	85 (57)[4]	72%[5]	152 (180)[6]
Squamous cell carcinoma	73%[1]	95 (60)[2]	0%	NA	0%	NA
Basal cell carcinoma	0%	NA	62%[3]	21 (13)[4]	98%[5]	236 (255)[6]

p values: [1]=1; [2]=0.22; [3]=0.16; [4]=0.0014; [5]=0.0043; [6]=0,0019

Figure 1 - 483

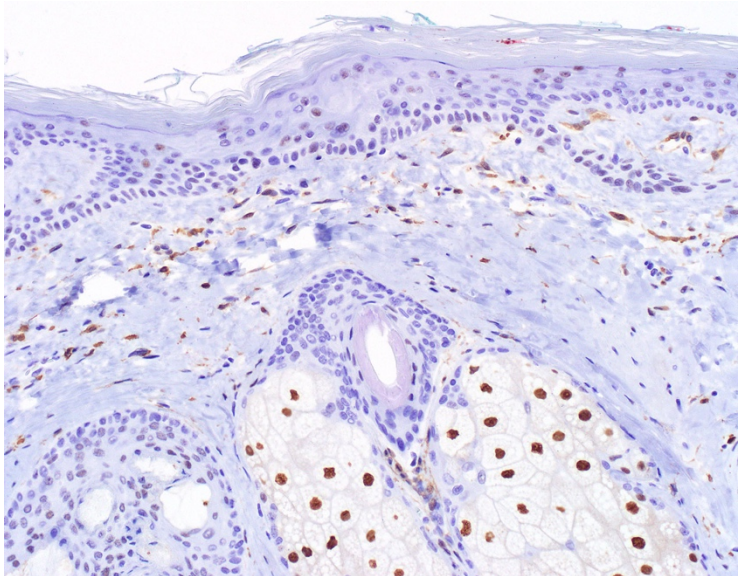

Conclusions: Factor XIIIa AC-1A1 positivity was seen in SEBC and SCC. For the differential of SEBC vs BCC, any factor XIIIa staining favors SEBC, while in the differential diagnosis of SEBC vs SCC, any AR staining favors SEBC. We affirmed the value of Ber-EP4 in the differential of BCC vs SCC, but highlighted frequent expression in SEBC.

484 Expression of p62/SQSTM1 in Melanoma and Tumor Microenvironment Correlates With BRAFV600E Expression in Tumor and Tumor Progression

Israel Kasago[1], Saleh Najjar[2], John Carlson[3]
[1]Albany Medical College, Delmar, NY, [2]Albany Medical Center, Albany, NY, [3]Albany Medical College, Albany, NY

Disclosures: Israel Kasago: None; Saleh Najjar: None; John Carlson: None

Background: p62/SQSTM1 plays a regulatory role in autophagy signaling cascades, a sequestration process that is variably influenced by BRAF mutational status and has been linked to therapeutic resistance in melanoma. Also, recent evidence indicates that a deficiency of p62 in the tumor microenvironment promotes tumorigenesis in prostate cancer. We evaluated the localization of p62 in melanoma and tumor microenvironment using immunohistochemistry, and correlated with BRAFV600E protein expression in the tumor.

Design: FFPE tissue sections from 102 melanomas to include in-situ were retrieved from the archive. The cohort consisted of 63 primary melanoma, 23 metastatic melanoma and 16 melanoma in situ. Tissue sections were immunostained using mouse monoclonal antibodies to p62/SQSTM1 and BRAFV600E (VE1). Cytoplasmic and nuclear p62 immunoreactivity was semiquantitatively assessed in the tumor (Cp62, Np62) and tumor microenvironment (Cp62 tm, Np62 tm), respectively. Scoring was based on staining intensity (weak, moderate, intense) and extent (focal <= 10%, regional 11-50%, diffuse >50%). Cytoplasmic BRAFV600E immunoreactivity in the tumor was scored as absent (0), weak (1), moderate (2), or intense (3). Staining results were correlated with clinicopathologic variables.

Results: Np62 expression was noted in 38/102 (37%) cases. Intense Np62 was noted in 17/38 (45%) tumors and the intensity correlated with tumor depth (0.3197, p= 0.0128), mitosis (0.3665, p= 0.0070) and AJCC 8th ed. TNM stage (0.3455, p= 0.0085). Cp62 expression was noted in 101/102(99%) of tumor. Intense Cp62 was noted in 9/102 (9 %) tumors and the intensity correlated with tumor infiltrating lymphocytes (-0.3280, p= 0.0165), tumor depth (0.2909, p=0.0241) and TNM stage (0.3208, p= 0.0150). Cp62tm and Np62tm was noted in 59/102 (58 %) and 43/102 (42 %) cases, and both correlated with tumor depth (-0.2646, p= 0.0410, 0.2845, p= 0.0276), respectively. BRAFV600E expression was noted in 45/102 (44 %) of tumors and inversely correlated with the extent of Cp62 (-0.2365, p= 0.0167).

Figure 1 - 484

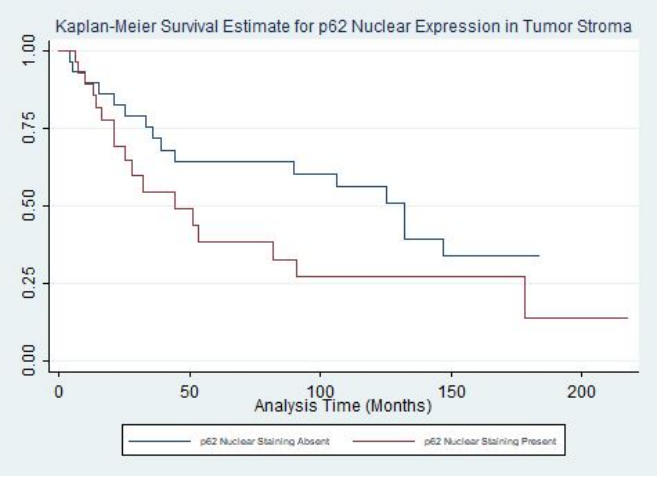

Figure 2 - 484

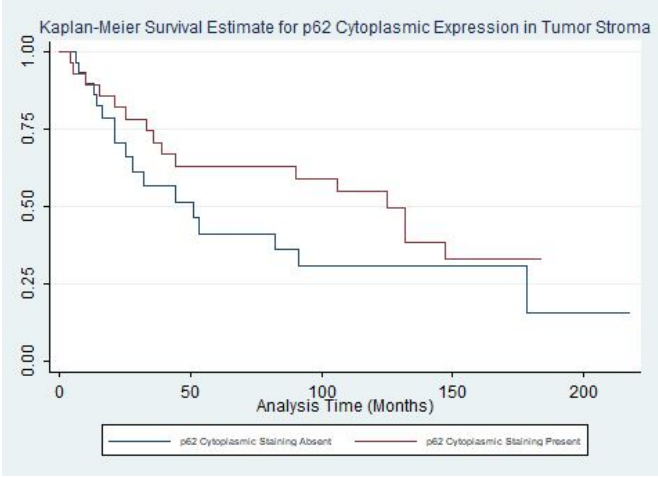

Conclusions: Cytoplasmic and nuclear overexpression of p62 was observed not only in the tumor cells but also in the tumor microenvironment of melanoma, and correlated with tumor progression and aggressive behavior. The inverse correlation between BRAF expression in the tumor and Cp62 extent confirms that BRAF mutational status correlates with activated autophagy system in melanoma. Targeting autophagy may be a potential adjuvant therapeutic option for melanoma.

485 Predicting BRAF and NRAS Mutations Using Deep Learning on Histopathology Images of Melanoma

Randie Kim[1], Sofia Nomikou[1], Zarmeena Dawood[1], Nicolas Coudray[1], George Jour[2], Una Moran[1], Narges Razavian[3], Iman Osman[4], Aristotelis Tsirigos[1]
[1]New York University School of Medicine, New York, NY, [2]NYU Langone Health, New York, NY, [3]New York University, New York City, NY, [4]New York University Medical Center, New York, NY

Disclosures: Randie Kim: None; Sofia Nomikou: None; Zarmeena Dawood: None; Nicolas Coudray: None; George Jour: None; Una Moran: None; Narges Razavian: None; Iman Osman: None; Aristotelis Tsirigos: None

Background: Identification of driver *BRAF* and *NRAS* mutations in melanoma has become a crucial component for the treatment of advanced or metastatic cases. While DNA molecular assays are the current gold standard to determine mutational status, they are costly and time-consuming. Deep Convolutional Neural Networks (CNN), a type of machine learning that utilize non-linear algorithms, have been successful in image analysis and classification on histopathological images of solid tumors. Here, we demonstrate that deep learning models can predict the presence of *BRAF* and *NRAS* mutations on histopathology images of melanoma.

Design: Primary melanomas diagnosed between 2002 to 2013 from 266 unique patients who provided consent in an IRB-approved clinicopathological database and melanoma biorepository were retrieved and divided into training, testing, and validation cohorts. In each cohort, *BRAF*-mutant, *NRAS*-mutant, and *WT/WT* melanomas were represented. The CNN Inception v3 was used to train for classifiers to select for regions containing melanoma and predict *BRAF* and *NRAS* mutational status on whole-slide histopathology images.

Results: Tumor-rich areas were initially manually annotated as regions of interest (ROI). The network was then trained on tiled images of manual annotated ROI only, with 70% of tiles used for training, 15% for validation, and 15% for testing. Model performance achieved a per slide Area Under the Curve (AUC) of 0.72 with a [0.57, 0.87] confidence interval (CI) for predicting mutated BRAF (Figure 1) and 0.72 CI [0.50,0.90] for predicting mutated *NRAS* (Figure 2). A fully automated model that pre-selects for ROI performed as well compared to annotation by a dermatopathologist. The predictive power of the network performed independently from available clinical data, such as age, histological subtype, and sex.

Figure 1 - 485

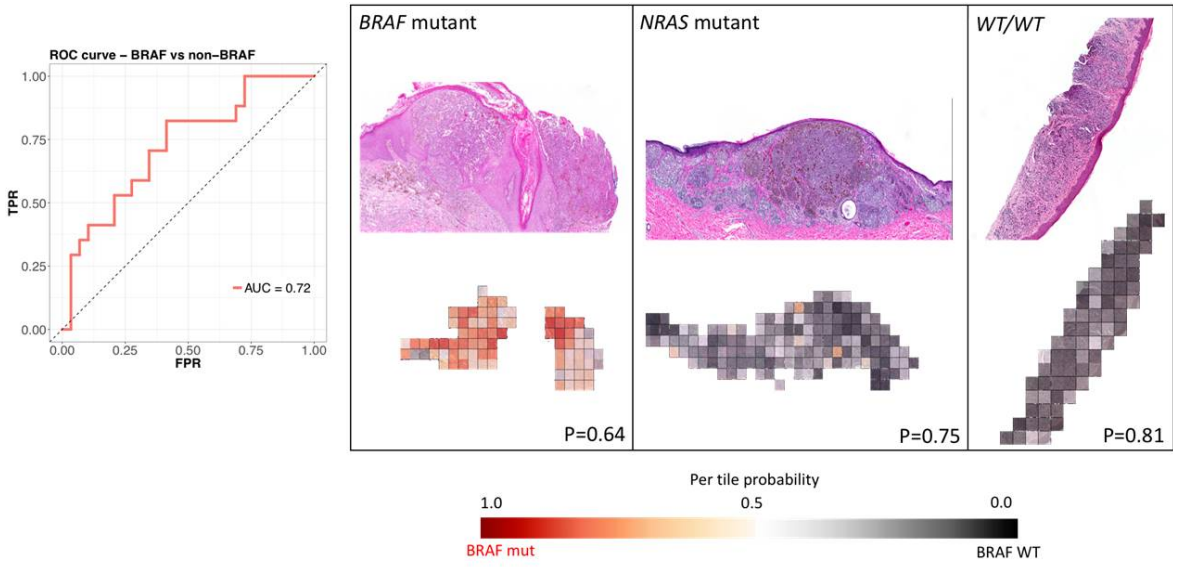

Figure 2 - 485

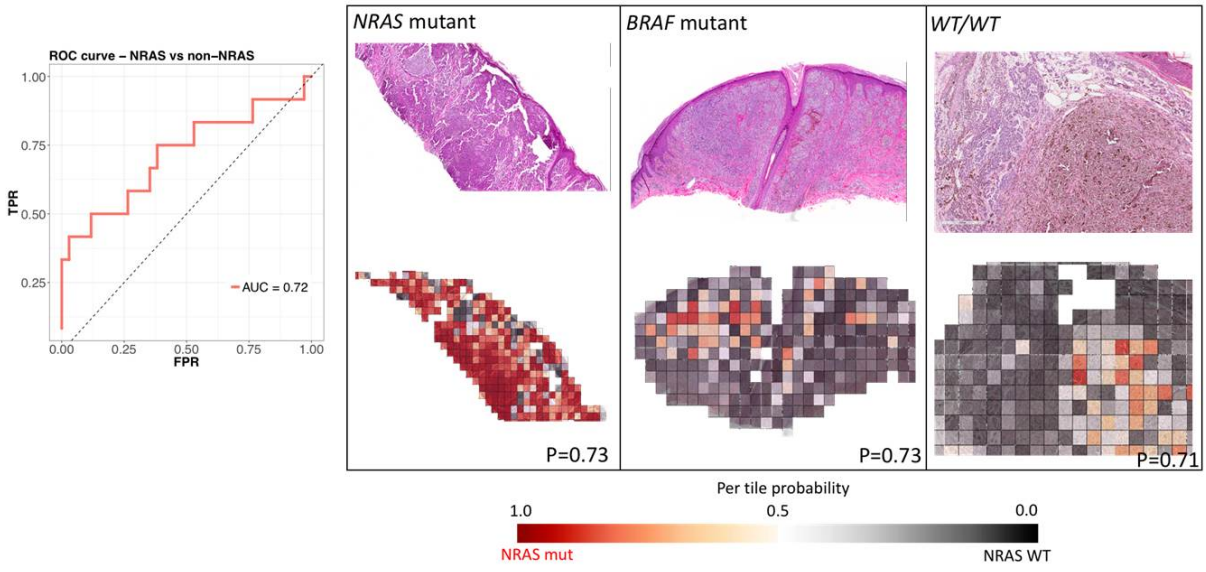

Conclusions: Application of deep learning is quickly being explored to aid cancer diagnosis and prognosis. We present a fully automated deep CNN model that accurately differentiates melanomas from benign tissue and uses morphologic features to predict the presence of *BRAF* or *NRAS* driver mutations. Model performance compared to existing screening assays, such as immunohistochemical detection of *BRAFV600E* are currently underway. Our approach has the potential to complement existing mutation determination assays with the purpose of significantly reducing costs, and importantly, expediting initiation of targeted therapy.

486 Immunoglobulin Gamma, Subclass 4 (IgG4) Expression in Cutaneous Marginal Zone Lymphoma (MZL)

Marsha Kinney[1], Olaoluwa Bode-Omoleye[2], Richard Wu[3], Kenneth Holder[4], Hongxin Fan[2], Edward Medina[1]
[1]The University of Texas Health Science Center at San Antonio, San Antonio, TX, [2]San Antonio, TX, [3]The University of Texas at San Antonio, San Antonio, TX, [4]The University of Texas Health Science Center at Houston, San Antonio, TX

Disclosures: Marsha Kinney: None; Olaoluwa Bode-Omoleye: None; Richard Wu: None; Kenneth Holder: None; Hongxin Fan: None; Edward Medina: None

Background: IgG4 expression has been reported in approximately 39% of cutaneous MZL (Brenner I et al, Mod Pathol 26:1568, 2013) but little clinical and pathologic information is known regarding IgG4+ cases. The purpose of this study is to compare the clinical and pathologic features of IgG4+ versus IgG4- MZL.

Design: 43 adult and 3 pediatric patients with 53 biopsies were tested for IgG4 expression and correlated with clinical, histologic, immunophenotypic and molecular features. Monotypic plasma cells (PC) had kappa:lambda ratios of K:L >5:1 or K:L of <1:2 or if Dutcher bodies (DB) were present. IgH rearrangement (IgHR) was performed using the BIOMED-2 FR1-3 and DH-JH primers.

Results: Overall 15/46 (33%) cases were IgG4+ (in 13/46 ≥50% of the PC were IgG4+ and in 2/46, 30%-49% of the PC were IgG4+). IgG4+ and IgG4- cases demonstrated similar age ranges, however, all three pediatric MZL were IgG4-. IgG4+ cases more often involved the trunk and less often the extremities. PC were IgG predominant in both IgG4+ and IgG4- cases; however, IgM+ or IgA+ Dutcher bodies were present in 52% of IgG4- cases versus 20% of IgG4+ cases. PC were monotypic by immunohistochemistry (IHC) in 13/15 (87%) and clonal by IgHR in 9/14 (64%) of IgG4+ cases and monotypic by IHC in 20/31 (65%) and clonal by IgHR in 21/31 (64%) of IgG4- cases. Combining IHC and IgHR, clonality was not detected in 1/15 (7%) IgG4+ cases and 6/31 (19%) IgG4- cases. Eosinophils were more often present in IgG4+ cases.

Parameter	IgG4+, 15 cases	IgG4-, 31 cases
M:F	8:7	18:13
Age range, years	29-82	9-78
Head/neck	4 (27%)	11 (35%)
Trunk	10 (67%)	13 (42%)
Extremities	1 (6%)	7 (23%)
B-cells >50%	8 (53%)	10 (32%)
Nodular component	10 (67%)	18 (58%)
FDC colonization	10 (67%)	17 (55%)
Weak BCL6 expression	15 (100%)	22 (71%)
Eosinophils present	12 (80%)	14 (45%)
IgG+ plasma cells predominant	15 (100%)	27 (87%)
IgA or IgM+ DB	3 (20%)	16 (52%)
Kappa+/Lambda+ plasma cells	7/6 (87%)	12/4/4 K+L+ DB (65%)
IgHR+/equivocal/neg/limited DNA	9/1/4/0	21/2/5/3
IHC-/IgHR-	1	6, 5 with IgA+ or IgM+ DB

Conclusions: Approximately 33% of MZL express IgG4 and >90% of IgG4+ cases occur on the trunk, head, or neck. IgG4+ MZL is more often B-cell rich, and eosinophils are present in small numbers in 80% suggesting the possibility of an origin in an antecedent bite response. While a majority of both IgG4+ and IgG4- cases show clonality, monotypic PC are more frequent in IgG4+ cases, however, Dutcher body formation is less frequent than in IgG4- cases. Interestingly, in IgG4+ MZL PC have almost equal kappa and lambda light chain distribution whereas the normal serum IgG4 K:L ratio is markedly biased at 8:1 (Finn WG et al., Am J Clin Pathol 146:303, 2016). Weak BCL6 expression is present in many cutaneous MZL and may be useful in establishing the diagnosis.

487 Syringocystadenoma Papilliferum of the Buttock, Vulva and Perianal Area Harbors Mostly BRAF V600 Mutations and are Associated in Some Cases with High-Risk HPV.

Liubov Kyrpychova[1], Anastasia M. Konstantinova[2], Jana Nemcova[3], Monika Sedivcova[3], Heinz Kutzner[4], Michal Michal[5], Dmitry Kazakov[6]
[1]Biopticka laborator s.r.o., Pilsen, Czech Republic, [2]Clinical Research and Practical Oncological Center, Saint-Petersburg, Russian Federation, [3]Biopticka laborator s.r.o., Plzen, Czech Republic, [4]Dermatopathologie Friedrichshafen, Friedrichshafen, Germany, [5]Biopticka Laborator SRO, Plzen, Czech Republic, [6]Biopticka Laborator SRO, Pilsen, Czech Republic

Disclosures: Liubov Kyrpychova: None; Anastasia M. Konstantinova: None; Jana Nemcova: None; Monika Sedivcova: None; Heinz Kutzner: None; Michal Michal: None; Dmitry Kazakov: None

Background: Syringocystadenoma papilliferum (SCAP) is a benign tumor most commonly involving the head and neck area occurring often in association with nevus sebaceus, where HPV DNA and mutations in the RAS/mitogen-activated protein kinase signaling pathway have been detected.

Design: We studied 16 patients (11 women and 5 men; age range 18 to 95 years; median 54 years; mean 52.9 years) with SCAP involving the buttock (43.8%), vulva (31.3%) and perianal area (25%), which are very rare locations. Histopathogic and molecular-genetic studies, including HPV PCR, *HRAS* and *BRAF V600* mutations were performed.

Results: Histopathologically, all tumors had a papillary architecture with the transition from the bilayered glandular epithelium to the keratinizing squamous epithelium with a dense plasma cell stromal infiltrate at the squamocolumnar junction. Other changes identified included prominent cystic alterations (18.8%), markedly exophytic areas with an arboreal growth pattern of the glandular elements (31.3%), wart-like changes (18.8%), various types of metaplasia (43.8%), hyperplasia of luminal cells resulting in cribriform structures (31.3%), focal hyperplasia of basal/myoepithelial cells (25%) and atypia in the squamous epithelium (7.7%). All 12 lesions stained immunohistochemically for p16 proved negative. HPV high-risk types (HPV16 and HPV68) was identified in 3 (23.1%) of the 13 analyzed cases. A missense mutation p.Gln61Arg in the proto-oncogene *HRAS* was found in 1 lesion (7.7%), whereas *BRAF V600* was detected in 8 of the studied 12 cases (66.7%).

Conclusions: SCAP located in the buttock and anogenital area manifests a spectrum of morphological changes similar to those seen in tumors in the head and neck area. Several neoplasm demonstrated features resembling those seen in warts but HPV DNA was not found. On the contrary, DNA of HPV high risk types were detected in some tumors without HPV-related morphology. Our study confirms the role of *HRAS* and *BRAF V600* mutations in the pathogenesis of SCAP, including SCAP in the anogenital areas and buttock, where BRAF V600 are more common.

488 Four-color Fluorescence In-situ Hybridization is Highly Sensitive and Specific to Distinguish Cutaneous Melanoma of Early Stage from Dysplastic Nevus

Zhong Wu Li, Peking University, Beijing, China

Disclosures: Zhong Wu Li: None

Background: It was usually challenging for pathologist to diagnose melanoma in early stage, especially to discriminate melanoma in situ from dysplastic nevus. Diagnosing melanoma with the help of four-color fluorescence in-situ hybridization(FISH) has been hot for years and proven to be effective. However, most of the previous studies were based on unambiguous lesions either malignant or benign, data about its significance to diagnose early-stage melanoma and dysplastic nevus was limited, probably because of limited cases of the two entities and of great difficulty to diagnose.

Design: 109 surgical excision specimens, including 51 cutaneous dysplastic nevi and 58 early-stage cutaneous melanomas, were conducted. And for all the melanoma cases, the Clark level was confined to no more than level 2. The gold standard to evaluate the sensitivity and specificity of FISH was determined by the histopathologic diagnosis from three experienced pathologists blinded to each other, and also blinded to the results of FISH. And for those discordant diagnosis, an agreement of two pathologists was considered to be the ultimate diagnosis.

Results: 50 Dysplastic nevi and 59 melanomas were confirmed finally. It manifested that several features were much more frequently observed in melanoma group, including more than 1 mitotic figures per square millimeter, pigmentation in stratum corneum, moderate-sever lymphocyte infiltration, moderate-sever cell atypia, and pagetoid growth pattern of melanocytes in epidermis. Besides, compared with that in the dysplastic nevus group, tumor size in the melanoma group was significantly larger and the age at diagnosis was much older.

The four-color FISH technology was highly sensitive and specific to distinct cutaneous melanoma from dysplastic nevus even in early stage, with the sensitivity 94.9%, the specificity 94.0%, the positive predictive value 94.9%, and the negative predictive value 94.0%. Moreover, 2 cases of melanomas misdiagnosed as nevus previously were turned out to be positive and 1 case of dysplastic nevus misdiagnosed as melanoma primarily to be negative in FISH detection.

We also found that Gaiser' criteria was relatively less sensitive and specific than Gerami's criteria (93.2% vs 94.9% for sensitivity, 90.0% vs 94.0% for specificity).

Figure 1 - 488

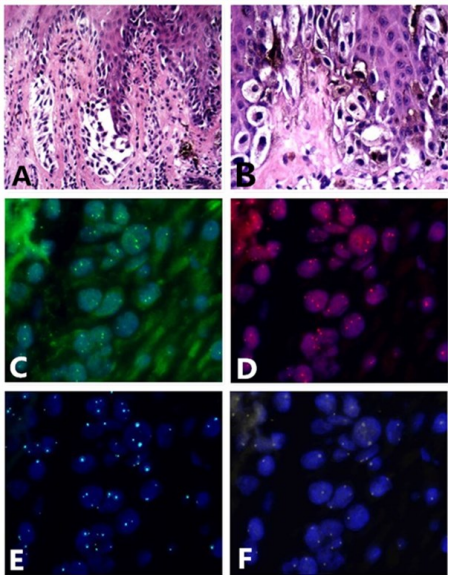

Figure 2 - 488

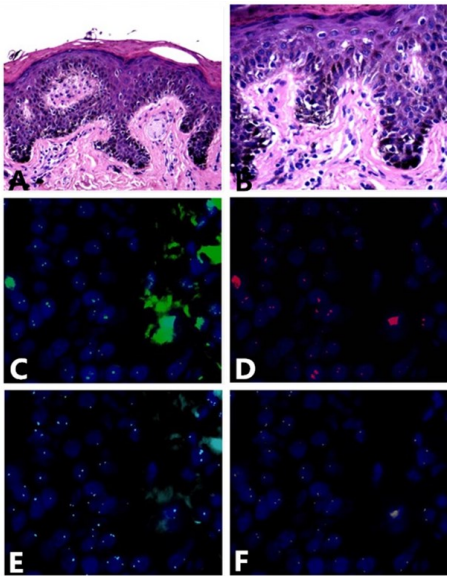

Conclusions: A combination of the four-color FISH test and histology was helpful to decrease the misdiagnosis rate of early stage melanoma and dysplastic nevus.

489 Comparison of Low-Coverage Whole Genome Sequencing (LCWGS) with Single Nucleotide Polymorphism (SNP) Based Chromosomal Microarray in the Diagnostic Work-up of Histologically Ambiguous Melanocytic Tumors

Valentina Logunova[1], Nicole Hoppman[1], Ross Rowsey[1], Lori Erickson[1], Thomas Flotte[1], Jean-Pierre Kocher[1], William Sukov[2], Katherine Geiersbach[1], Chen Wang[3], Ruifeng Guo[2]
[1]Mayo Clinic, Rochester, MN, [2]Rochester, MN, [3]Mayo Clinic College of Medicine, Rochester, MN

Disclosures: Valentina Logunova: None; Ross Rowsey: None; Lori Erickson: None; Thomas Flotte: None; William Sukov: None; Katherine Geiersbach: None; Chen Wang: None; Ruifeng Guo: None

Background: Histologically ambiguous melanocytic tumors are among the most challenging in dermatopathology practice. Molecular cytogenetic analysis of such lesions is increasingly used to support the diagnosis, predict biologic behavior, and provide treatment guidance. Chromosomal microarray and FISH are the two most common methods for detection of chromosomal aberrations in melanocytic lesions. Newer SNP microarray assays are increasingly used to replace traditional array comparative genomic hybridization. The aim of our study is to compare a novel LCWGS assay to SNP microarray as an alternative with similar performance for detecting chromosomal abnormalities and potentially better cost-effectiveness and shorter turn-around-time (TAT).

Design: The study cohort included 24 cases of borderline melanocytic tumors from our Dermatopathology consultative service. The morphological features were classified into the following groups: Spitz-like (n=11), deep penetrating nevus-like (n=3), blue nevus-like (n=3), nevoid (n=5), unclassifiable (n=2). DNA was extracted from formalin fixed paraffin embedded tissue from each case and analyzed by a commercially available SNP array platform (Affymetrix Oncoscan V3) and a laboratory developed LCWGS assay with a bioinformatics pipeline validated for non-invasive prenatal screening.

Results: Oncoscan successfully resulted in 23 cases, with one case failed due to insufficient DNA. LCWGS was able to result in all 24 cases. Both Oncoscan and LCWGS demonstrated 11 cases with copy number aberrations. Overall, 14 gains and 15 losses were detected by both methods with a concordance rate of 100%. The other 12 cases had normal results by both methods. The failed Oncoscan case showed a normal result with LCWGS. One case had loss of heterozygosity (LOH) which was only detected by Oncoscan; LCWGS lacks the capacity to detect this abnormality. The wet bench and analytic phase takes 3 days for Oncoscan and 24-30 hours for LCWGS. The cost of LCWGS is 30-50% that of Oncoscan.

Figure 1 - 489

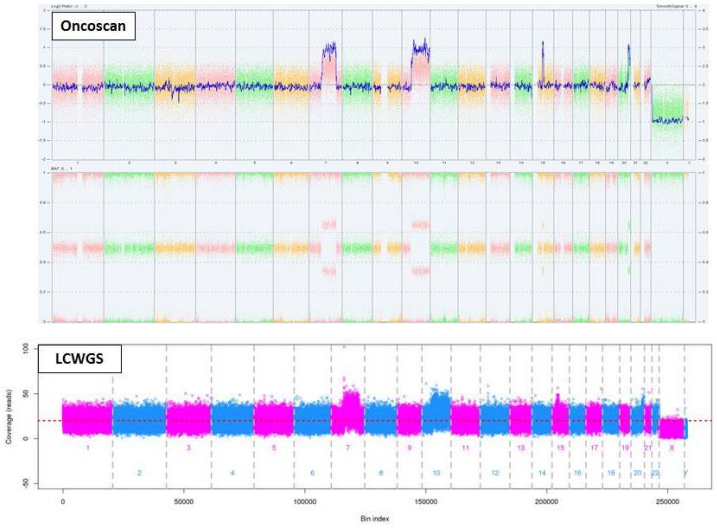

Figure 1. Oncoscan and LCWGS demonstrating gain of 7q, 10q, 15q, and 20q in one example case

Conclusions: LCWGS is a robust molecular test to detect chromosomal aberrations and assist in diagnosis of ambiguous melanocytic tumors, and its performance is at least comparable to Oncoscan-based SNP array. LCWGS is potentially more cost-effective and provides shorter TAT. The main challenge of LCWGS is its inability to detect LOH, which can be overcome with the addition of targeted analysis. Future larger-scale controlled studies are needed.

490 MAP3K8 Rearrangements Are Recurrent in Spitzoid Melanoma and Correlate with a Distinct Morphologic Phenotype

Scott Newman[1], David Ellison[2], Alberto Pappo[2], Armita Bahrami[1]
[1]St. Jude Children's Research Hospital, Memphis, TN, [2]St. Jude Children's Research Hospital, Memphis, TN

Disclosures: Scott Newman: None; David Ellison: None; Alberto Pappo: None; Armita Bahrami: None

Background: Spitzoid melanoma is a distinct and morphologically heterogeneous variant of melanoma that more commonly affects children and adolescents, and is a subtype considered as low-grade or borderline on the spectrum of malignancy. The genomic profile of spitzoid melanoma is also distinct from the adult (conventional melanoma) counterpart. Unlike adult melanoma, where activating mutations in BRAF or NRAS, or inactivating mutations in NF1, are observed in most cases, the driving oncogene for 40-50% of spitzoid melanoma is a kinase fusion involving ALK, NTRK1/2/3, ROS1, RET, BRAF, or MET. In the remaining cases, however, no driving kinase fusion or mutation has yet been identified.

Design: We analyzed a cohort of 49 formalin-fixed paraffin-embedded tumor samples (36 spitzoid melanomas; 13 atypical Spitz tumors) from 49 patients ranging in age from 2 to 28 years (median, 9) by RNA-sequencing using methods described previously. Gene fusions and coding mutations at cancer hotspots were detected using our previously described bioinformatics pipeline.

Results: We detected the previously described fusions of ALK, NTRK1, NTRK3, BRAF, RAF1, ROS1, and RET collectively in 21 of 49 patients (43%), and novel in-frame fusions or C-terminal truncations of MAP3K8, a serine−threonine kinase that activates MEK, in 17 of 49 patients (34%). MAP3K8 fusions or truncations were mutually exclusive of other fusions and were found in both spitzoid melanoma (n=16) and atypical Spitz tumor (n=1). Tumors with MAP3K8 disruptions came from 10 female and 7 male patients, ranging from 2 to 18 years of age (median, 6), and arose in the upper extremity (n=5), lower extremity (n=5), trunk (n=4), and head & neck (n=3). In 85% of patients, the clinical diagnosis was a non-melanocytic lesion. Tumors with MAP3K8 were morphologically distinct, generally characterized by a compound proliferation of large cells with epithelioid phenotype and abundant cytoplasm, arranged in syncytial aggregates or confluent nests. Ulceration was found in 53% (9/17), loss of p16 by immunohistochemistry in 82% (14/17), and biallelic loss of p16 by FISH in 70% (12/17). Sentinel lymph nodes were positive for disease in 72% in the entire cohort, and in 67% of patients with MAP3K8-rearranged tumors. In the entire cohort, only one patient with MAP3K8-rearranged tumor developed distant metastasis and died of disease.

Conclusions: MAP3K8 disruptions are highly recurrent in spitzoid melanoma and define a distinct morphologic phenotype in spitzoid tumors.

491 Inactivating Mutations in NF1 are Frequent in Naïve Untreated Primary Cutaneous Melanomas with a Negative Sentinel Lymph Node

Kei Shing Oh[1], Meera Mahalingam[2]
[1]St. George's University, St George Grenada, Grenada, [2]VA Integrated Service Networks (VISN1), Brookline, MA

Disclosures: Kei Shing Oh: None; Meera Mahalingam: None

Background: Sentinel lymph node [SLN] biopsy, a technique that evaluates the first/draining node of the primary melanoma is typically offered to all patients with a primary melanoma >1 mm in depth. However, using this cut-off, not all melanomas exhibit a positive SLN. Given this, our primary aim was to characterize alterations in cancer-relevant genes in primary cutaneous melanomas [PCMs] with a negative SLN. The control group included PCMs with a positive SLN. An additional aim was to assess for intertumoral heterogeneity by comparing the genotype of matched PCM with matched metastases or multiple metastases from the same primary.

Design: PCMs with a negative SLN and PCMs with matched metastases and multiple metastases from the same primary with enough tissue for genetic analyses met criteria for inclusion in this study. An augmented, enrichment-based, next-generation sequencing assay was used on archived formalin-fixed paraffin-embedded tissue samples of the following:
Group 1 = PCMs with a negative sentinel lymph node [n=8]
Group 2 = Paired primary cutaneous melanomas [PCMs] with a positive SLN or multiple metastases from the same primary [n=6]

Results: In Group 1: The mean number of mutations was 40 (range 3-71) with the most frequent mutation in *NF1*(100% of cases) followed by *GNAS, KNT2A, MECOM*and *ROS1*(75% of cases), *AR1D1A, ERB4, FLT4, PDGFRB* and *TP53*(62.5% of cases) and *ESR1, FLT1, NTRK3, ROS1*and *TSC1*(50% of cases). In Group 2: The mean number of mutations was 10 (range 5-19) with the most frequent mutation (60% of cases) in *MET*and *BRAF (V600R*and *V600K*) followed *by ABL1, AKT2, AR1D1A, CCNE1, MECOM, NF1, NRAS* and *RET*(40% of cases) with additional unique mutations noted in all 6 matched samples.

Conclusions: Our findings indicate that inactivating mutations in *NF1* are extremely frequent in naïve untreated PCMs with a negative SLN. Loss of neurofibromin function results in increased signaling through the *RAS* pathway and downstream MAPK and mTOR pathways. Given this, the obvious clinical implication is that patients in this subgroup may be sensitive to mTOR inhibitors and MAPK pathway inhibitors, several of which are currently FDA-approved. The presence of additional mutations in matched samples suggests that this may contribute to failed targeted therapy. Larger series of cases are required to confirm our findings.

492 Filaggrin Expression via Immunohistochemistry as a Marker of Differentiation in Squamous Cell Carcinoma

Christine Orr[1], Kaitlin Vanderbeck[2], Nikoo Parvinnejad[3], Ami Wang[1], Tao Wang[2], Yuka Asai[4]
[1]Kingston, ON, [2]Queen's University/Kingston Health Sciences Centre, Kingston, ON, [3]University of Alberta, Edmonton, AB, [4]Kingston Health Sciences Centre, Kingston, ON

Disclosures: Christine Orr: None; Kaitlin Vanderbeck: None; Nikoo Parvinnejad: None; Ami Wang: None; Tao Wang: None; Yuka Asai: None

Background: Filaggrin is a protein integral to the structure and barrier function of the epidermis. Expressed in the granular layer, filaggrin loss-of-function mutations are present in 10% of the North American population and increase the risk of developing atopic dermatitis and ichthyosis vulgaris. Prior small studies have investigated the use of filaggrin immunohistochemistry (IHC) to differentiate benign, premalignant and malignant skin neoplasms of mixed phenotypes; however, the use of filaggrin IHC staining patterns in squamous cell carcinomata (SCC) has not yet been studied.

Design: Tissue microarrays (TMA) were created from 216 cases of formalin-fixed paraffin-embedded SCC cases obtained at our institution (two 0.6 mm cores each at 1.0 mm spacing). Cases were stained with optimized anti-filaggrin antibody (FLG01, 1:200, monoclonal mouse) and were evaluated for filaggrin expression (normal, abnormal, or negative) by three independent pathologists (Figure 1). “Normal” was defined as superficial granular expression. “Abnormal” was defined as diffuse expression. “Negative” lacked expression. Final statistical analysis was completed by Fisher Exact Test.

Results: 196 SCC cases were evaluated: 82 well-differentiated (WD), 90 moderately-differentiated (MD), and 24 poorly-differentiated (PD) cases (Table 1). The absence of filaggrin expression in SCC tumors was significantly increased in PD cases when compared to WD ($p<0.0001$) and MD ($p=0.0231$) cases; and in MD cases when compared to WD ($p=0.0099$). Abnormal staining was significantly increased in PD cases when compared to WD cases ($p=0.0039$); and in MD cases when compared to WD cases ($p=0.0006$).

Table 1. Absolute number of cases exhibiting pattern of filaggrin IHC staining.			
	Pattern of IHC Staining		
Differentiation	*Normal (%)*	*Abnormal (%)*	Absent (%)
Well	30 (37)	32 (39)	20 (24)
Moderate	12 (13)	51 (57)	27 (30)
Poor	0 (0)	10 (42)	14 (58)

Figure 1 - 492

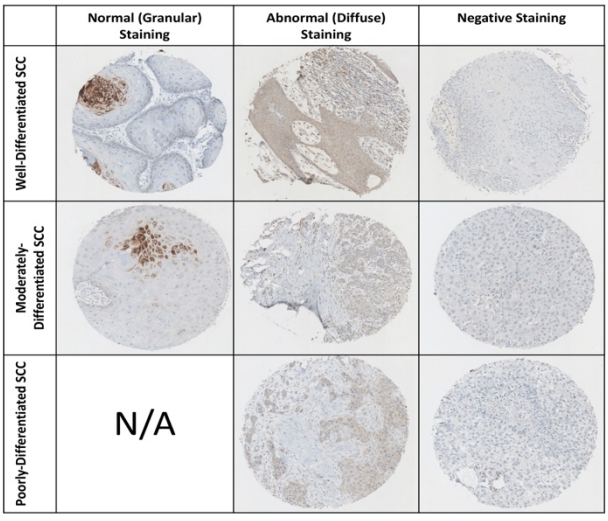

Figure 1: Examples of filaggrin expression patterns in well, moderate, and poorly-differentiated squamous cell carcinoma.

Conclusions: Our findings of abnormal filaggrin expression in poorly and moderately differentiated SCC via IHC may support the use of filaggrin in limited biopsies when differentiation is not easily determined. Furthermore, filaggrin mutations in SCC may be linked to loss of differentiation in SCC and thereby be associated with a worse prognosis. This potential relationship of filaggrin expression to SCC prognosis may be further elicited with future studies investigating filaggrin expression in SCC cases with and without metastasis.

493 SOX-10 Immunostaining as a Potential Diagnostic Pitfall in the Evaluation of Fibromatosis and Cutaneous Scar

Anthea Paul[1], Stephanie Petkiewicz[2], Bibianna Purgina[3], Denis Gravel[4], Susan Robertson[5]
[1]The Ottawa Hospital - University of Ottawa, Ottawa, ON, [2]University of Massachusetts, Ottawa, ON, [3]University of Ottawa/The Ottawa Hospital, Ottawa, ON, [4]Ottawa Hospital, Ottawa, ON, [5]The Ottawa Hospital, Ottawa, ON

Disclosures: Anthea Paul: None; Stephanie Petkiewicz: None; Bibianna Purgina: None; Denis Gravel: None; Susan Robertson: None

Background: SOX-10 immunostaining is useful in the work-up of desmoplastic melanoma.Recently, occasional SOX-10 positive cells in scar has been described.We have noted scattered SOX-10 positive spindle cells in fibromatosis.Because of our concerns of a potential pitfall of SOX-10 expression in fibromatosis, we examined SOX-10 expression in previously diagnosed cases of fibromatosis, desmoplastic melanoma, and cutaneous scars in our institution.Herein, we describe these findings, which could be potential diagnostic pitfall, especially in small biopsy samples.

Design: A total of 17 cases of fibromatosis and as controls, 9 cutaneous scars and 8 desmoplastic melanomas were retrieved from archives.The formalin-fixed paraffin embedded tissue was immuno-stained with SOX-10 (Biocare, Pacheco, CA, USA; clone BC34, 1:100).The amount and intensity of staining was quantified digitally using 500 cell hotspots.Statistical analysis was performed using Welch's ANOVA and Games-Howell post hoc analysis.

Results: The mean percentage of SOX-10 positive cells in a 500 cell hotspot was statistically different between the fibromatosis (5.2), desmoplastic melanoma (66.9), and scar groups (2.9) (Welch's F(2, 14.411)= 22.643, p <0.005)).The percentage of SOX-10 positive cells in a 500 cell hotspot was significantly higher in the desmoplastic melanoma group (66.9 +/- 27.0) than in the scar and fibromatosis groups (5.2 +/- 4.5 and 2.9 +/- 1.9 respectively).Games-Howell post hoc analysis revealed the mean differences between the melanoma and scar groups was statistically significant (61.7, 95% CI [33.6 to 89.8]; p=0.001) as was the difference between the desmoplastic melanoma and fibromatosis groups (64.0, 95% CI [35.9 to 92.1]; p=0.001).Statistical significance was not noted between the scar and fibromatosis groups (2.32, 95% CI [-0.87 to 5.51]; p=0.18).

Diagnostic Entity	Number of Cases	Average % of SOX-10 staining in hotspot	Most common pattern of SOX-10 staining
Fibromatosis	17	5.2	Rare scattered cells
Desmoplastic melanoma	8	66.9	Diffuse
Cutaneous scar	9	2.9	Rare scattered cells

Conclusions: Our data illustrates SOX-10 as a useful tool in discerning staining patterns among these 3 diagnostic entities.Although SOX-10 staining is seen in fibromatosis, the percentage of positive staining cells is significantly less than in desmoplastic melanoma and the pattern of positive cell distribution is different.SOX-10 staining in desmoplastic melanoma is diffuse, whereas the SOX-10 positive spindle cells in fibromatosis and cutaneous scar tend to be rare scattered cells.The SOX-10 staining patterns are similar for fibromatosis and cutaneous scar.Awareness of these staining patterns can avoid the potential diagnostic pitfall and incorrect diagnosis of desmoplastic melanoma.

494 Acral Pigmented Spindle Cell Nevus: Histopathologic Analysis in a Series of 21 Cases

Nathan Paulson[1], Gauri Panse[2]
[1]Yale University School of Medicine, New Haven, CT, [2]Yale University, New Haven, CT

Disclosures: Nathan Paulson: None; Gauri Panse: None

Background: Pigmented spindle cell nevus (of Reed) (PSCN) is a melanocytic nevus with distinct features that occurs most commonly on the proximal lower extremities of young females and may clinically and histologically mimic melanoma. PSCN occurring on acral sites are uncommon and not well-characterized. We sought to expand the clinicopathologic spectrum of PSCN by evaluating histologic features in a large series of acral PSCN.

Design: All PSCN from acral sites seen at our institution between 2000 and 2018 were reviewed and the clinical and histologic features were recorded. T-tests and Fisher's exact tests were used to determine statistical significance of differences in these features in upper extremity versus lower extremity lesions.

Results: Twenty-one acral PSCN cases were identified out of 490 total PSCN (4.3%). The average patient age was 27.5 years (range 3-69 years). Acral PSCN were more common in males (n=13) than in females (n=8). Thirteen of the cases were on the foot and 8 were on the hand. The clinical impressions included atypical nevus, pigmented Spitz nevus and melanoma. Out of the total 21 cases, 17 were junctional lesions and four of the lesions had a dermal component, which averaged 0.47 mm in depth. No dermal mitoses were identified. Average size of a lesion was 3.6 mm (range 1.4 to 7.6 mm). PSCN occurring on the feet were larger in size than those from the hands (p=0.037). Circumscription was seen in all cases, although lentiginous proliferation, pagetoid scatter, and nest variation were found in 17, 16 and 8 cases, respectively. Adnexal involvement was seen in 8 cases and Kamino bodies were identified in 6. Lymphocytic infiltrate was present in 8 lesions (including a dense infiltrate in 4 cases) all of which occurred on the lower extremity lesions (p=0.0068).

Conclusions: Acral PSCN are uncommon and constitute <5% of all PSCN. PSCN from acral sites may not display the traditional gender predilection of non-acral sites. Lesions seen on acral sites frequently demonstrate a lentiginous proliferation of melanocytes as well as variation in the nest size but are typically well-circumscribed. Lower extremity acral lesions tend to be larger and are more frequently associated with a lymphocytic infiltrate. It is important to be aware of the histologic features of PSCN occurring on acral sites to allow its distinction from acral melanoma.

495 WT-1: a Useful Marker for Distinguishing Cutaneous Atypical Vascular Lesions (Benign Lymphangiomatous Papules and Plaques) from Angiosarcoma

Ifeoma Perkins[1], Anders Meyer[2], Steven Billings[3], Philip LeBoit[1]
[1]University of California, San Francisco, San Francisco, CA, [2]Cleveland Clinic, University Heights, OH, [3]Cleveland Clinic, Cleveland, OH

Disclosures: Ifeoma Perkins: None; Anders Meyer: None; Steven Billings: None; Philip LeBoit: None

Background: Lymphatic-type atypical vascular lesions (AVLs), also known as benign lymphangiomatous papules and plaques (BLAPs) of the skin, are difficult to distinguish from cutaneous angiosarcomas. WT1 is a zinc finger DNA-binding transcription factor essential for the normal development of the genitourinary tract, hematopoiesis, and angiogenesis. Overexpression of the protein has been reported in a variety of cutaneous vascular proliferations including pyogenic granuloma (lobular capillary hemangioma), hemangiomas, glomus tumors, Kaposi sarcoma, and angiosarcoma. Recent studies report WT1 to be negative in cutaneous vascular malformations, aiding in their histopathologic distinction from hemangiomas. However, the expression profile of WT1 in AVLs is currently still unknown.

Design: We identified cases of cutaneous AVLs and a control group of cutaneous or soft tissue angiosarcoma from the databases of two high-volume referral centers. All cases of AVL with available slides were reviewed, including clinical and treatment history, patient demographics, and available histopathology. All cases with available tissue blocks were stained for WT1.

Results: Ten cases of AVL from 8 patients were identified; 12 angiosarcomas served as controls. The 8 patients with BLAPS were all middle-aged adult females (range 44-82 years; mean: 56 years). Of those with available clinical history, 100% (7 of 7) with AVLs had a history of breast cancer, most of which were also reported to have been treated with external beam radiation therapy (5 of 7, 71%). AVLs occurred on the breast (9 of 10; 90%) or axillae (1 of 10; 10%). Of those with available histories, 8% (1 of 12) of the angiosarcoma cohort had a history of external beam radiation therapy to the affected site. WT-1 was negative in 10 of 10 (100%) cases of AVL. Conversely, 11 of 12 (92%) cases of angiosarcoma stained positively for WT1 exhibiting cytoplasmic (11 of 11; 100%), perinuclear dot (Golgi) (9 of 11; 82%), and nuclear (7 of 11; 64%) staining patterns.

Conclusions: We conclude that WT1 is consistently negative in cutaneous AVLs and positive in angiosarcomas. As such, WT1 is a reliable ancillary tool useful in distinguishing AVLs from angiosarcoma.

496 Next Generation Sequencing (NGS)-Based Molecular Characterization of Conjunctival Melanoma

Dinesh Pradhan[1], Arivarasan Karunamurthy[2], Raja Seethala[3], Cindy Sander[2], Somak Roy[2], John Kirkwood[2], Uma Rao[4]
[1]The University of Texas MD Anderson Cancer Center, Houston, TX, [2]University of Pittsburgh Medical Center, Pittsburgh, PA, [3]University of Pittsburgh School of Medicine, Pittsburgh, PA, [4]UPMC, Shadyside Campus, Pittsburgh, PA

Disclosures: Dinesh Pradhan: None; Arivarasan Karunamurthy: None; Raja Seethala: None; Cindy Sander: None; Somak Roy: None; John Kirkwood: None; Uma Rao: None

Background: Conjunctival melanoma (CM) is an unusual, highly aggressive malignancy with poor prognosis. Metastasis occurs in around 30% of patients in 3 years and the 10-year disease-specific mortality is 9–35%. CM is inherently distinct from other mucosal, uveal and cutaneous melanomas; however the molecular pathogenesis of CM is poorly understood hindering the development of targeted therapy.

Design: Eight conjunctival melanomas and 3 benign conjunctival nevi (CN) were retrieved from the pathology archives at a large academic medical center after IRB approval. Formalin-fixed, paraffin embedded tissue sections were used for tumor microdissection. Extracted DNA was sequenced using customized targeted 32 gene panel on the Ion Torrent/Proton platforms (Thermo Fisher Scientific Inc.). Bioinformatics analyses were performed using Torrent Suite and custom developed software suite.

Results: The median age of the CM and CN patients was 83.5 years (range 53-96) and 52 years (range 31-56), respectively. The M: F ratio was 1:3 and 2:1 for CM and CN, respectively. The mean lesion size was 1.5 mm. All 3 CNs harbored activating *NRAS* codon 61 mutations (Q61R, Q61K and Q61K). All CMs demonstrated at least one pathogenic mutation (figure 1) and two cases had 3 or more mutations. Genomic alterations in *EIF1AX* (N4Y) and *NRAS* (Q61h & Q61R) were the most frequent. Additional mutations included *BRAF* (S467L), *EGFR* (M600T), *PDGFRA* (D576N), *MET* (R988C), *ATM* (V410M), *NF1* (L1187F), *ERBB4* (E928V), *GRIN2A* (D369N), *PREX2* (E414K) and *STK19* (D89N). Interestingly, activating mutations in *BAP1, KIT, SF3B1, GNAQ, GNA11* and *BRAF* V600E were not identified in any of the studied cases.

Figure 1 - 496

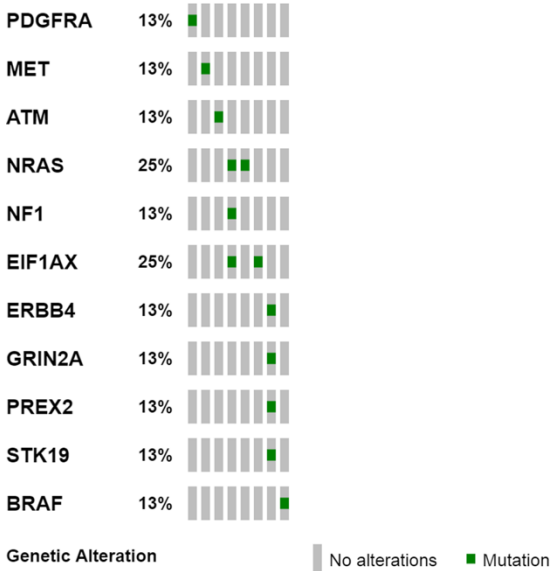

Conclusions: Mutational analysis of CM reveals a distinct mutational profile from uveal and other mucosal melanomas and shows some similarity to cutaneous melanomas. Similar *NRAS* mutations in CNs and some CMs suggest a possibility of common precursor pathway among a subset of these lesions. Molecular profiling of CM may be valuable in strategizing management in metastatic CMs with therapeutically actionable alterations such as *NRAS, NF1, BRAF, PDGFRA, ERBB4* and *EGFR*.

497 Abstract Withdrawn

498 Fat Necrosis with an Associated Lymphocytic Infiltrate Represents a Histopathologic Clue that Distinguishes Cellular Dermatofibroma from Dermatofibrosarcoma Protuberans

Shula Schechter[1], Rajiv Patel[1]
[1]*University of Michigan, Ann Arbor, MI*

Disclosures: Shula Schechter: None; Rajiv Patel: None

Background: Cellular dermatofibroma (CDF) and dermatofibrosarcoma protuberans (DFSP) can be challenging to differentiate from one another. Morphologically, both entities commonly extend into the subcutis, exhibit high cellularity with limited cytologic atypia and have a mixed fascicular-to- storiform growth pattern. In contrast to CDF, IHC of DFSP shows an absence of factor XIIIa and strong diffuse positivity for CD34 in most cases. However, CD34 positivity occurs in up to 25% of CDF, while 20% of DFSP lack significant CD34 expression. CD34-positive dermal fibroblasts at the periphery of CDF and factor XIIIa positivity in dermal dendrocytes in DFSP may confound interpretation. We sought to evaluate the significance of fat necrosis with an associated lymphocytic infiltrate as a histopathologic clue for distinguishing CDF from DFSP, in conjunction with other histopathologic features.

Design: We identified cases in our pathology database with a primary diagnosis of CDF or DFSP that were made between 2008 and 2017. Punch or excisional biopsy specimens with extension into the subcutis were selected. Previously biopsied lesions and specimens that did not interact with the subcutis were excluded. Histopathologic features were evaluated in hematoxylin and eosin stained sections. Data were analyzed by Chi square.

Results: Cases with at least 3 of the noted features (Table 1) were reliably identified as CDF whereas cases with fewer than 3 features were invariably diagnosed as DFSP (p=0.000000). Honeycombing was more common in DFSP (11/14 vs. 1/18 with CDF; p. = 0.000023). The presence of floret like giant cells, Grenz zone, epidermal hyperplasia, and hemosiderin laden cells did not statistically differentiate CDF from DFSP. FXIIIa was strongly positive in 16/18 CDF cases and in 0/10 DFSP cases whereas CD34 was focally positive in 10/18 CDF cases and diffusely positive in 13/14 DFSP cases. The presences of fat necrosis in association with a lymphocytic infiltrate were the most useful histologic features for distinguishing CDF from DFSP.

Table: Histopathological features distinguishing CDF and DFSP are shown below.

Feature	CDF	DFSP	p value
Fat necrosis with associated lymphocytic infiltrate	18/18	0/14	0.000000
Fat necrosis	18/18	3/14	0.000003
Lesional lymphocytes	15/18	3/14	0.0005
Collagen trapping present	18/18	9/14	0.006

Figure 1 - 498

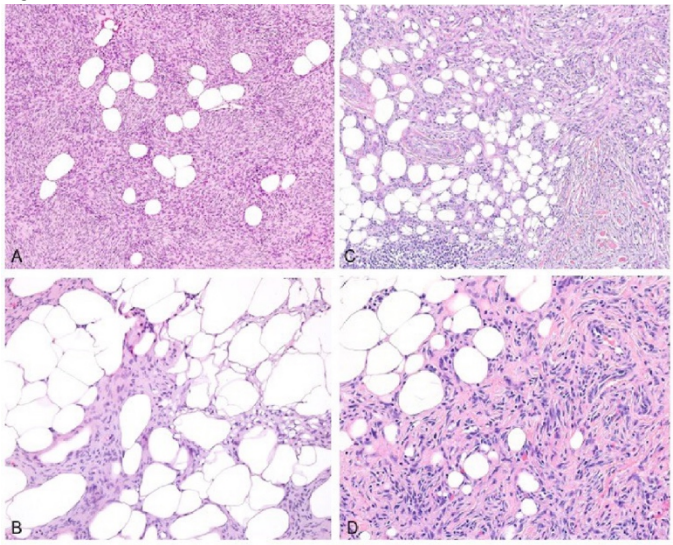

Figure 1. Representative H&E of DFSP and CDF. A, DFSP with "honeycomb" infiltration of fat without necrosis or inflammation. B. DFSP with fat necrosis without lymphocytic infiltrate. C and D. CDF with fat necrosis and associated lymphocytic infiltrate.

Conclusions: Fat necrosis with an associated lymphocytic infiltrate represents a useful histopathologic clue that distinguishes CDF from DFSP in cases were infiltration of the subcutis is present, particularly when IHC results are confounding. Our series represents the first report of the usefulness of this histopathologic clue in the differential diagnosis of CDF vs. DFSP.

499 Anaplastic Lymphoma Kinase – Wild Type Overexpression in Merkel Cell Carcinoma

Vishnu Vardhan Serla[1], Kabeer Shah[2], Rory Jackson[1], Hao Xie[1], Aaron Mansfield[1], Thomas Flotte[1], Kevin Halling[2]
[1]Mayo Clinic, Rochester, MN, [2]Rochester, MN

Disclosures: Vishnu Vardhan Serla: None; Kabeer Shah: None; Rory Jackson: None; Hao Xie: None; Aaron Mansfield: *Advisory Board Member*, Genentech; *Advisory Board Member*, AbbVie; *Advisory Board Member*, Bristol-Meyers Squibb; *Grant or Research Support*, Novartis; *Grant or Research Support*, Verily; Thomas Flotte: None; Kevin Halling: None

Background: Merkel cell carcinoma (MCC) is an aggressive skin tumor commonly seen in the adult population. Anaplastic lymphoma kinase oncogene (ALK) has been shown to be overexpressed in MCC by Quantitative RNA expression analysis and could potentially be a therapeutic target. The mechanism and clinical significance of ALK overexpression is currently unknown. Herein we evaluate a clinically annotated cohort of patients with MCC and attempt to further understand the mechanism of overexpression of the ALK oncogene.

Design: A clinically annotated cohort of 65 formalin-fixed, paraffin-embedded (FFPE) MCC cases were cut at 5 microns and subsequently isolated for total RNA using the RNeasy FFPE kit (Qiagen Cat: 73504). The RNA was input (200 ng) into a custom built NanoString Elements assay designed to distinguish between wild type (WT) ALK, gene fusion rearranged ALK, and an alternative transcript of ALK (ALK-ATI) which initiates transcription in intron 19 of ALK. The three forms of ALK were distinguished through the use of probes to the proximal, intron 19, and distal portions of the gene. With this probe set, WT ALK should show roughly equal expression of the probes for all three regions, ALK-ATI should show roughly equal expression of the intron 19 and distal probes and little expression of the proximal probes, and ALK fusion cases should show expression of the distal probes with little if any expression of the proximal and intron 19 probes. Each case was also stained for ALK protein (ALK D5F3 XP Rabbit mAb#3633, Cell Signaling Technology) for comparison purposes.

Results: Data from 65 Patients with MCC (age 73.8 ± 12 years, F/M 21/44) were analyzed. Analysis performed through Nanostring revealed 59 patients overexpressed ALK and 6 had no expression of ALK. Of these 59 patients, 52 had ALK-WT overexpression, 1 had some ATI mixed in, but mostly WT and 6 patients showed some expression but were not recognized as ALK WT overexpression. There was no association found between ALK overexpression and patient characteristics including age, gender, tumor site, and survival. However patients with high intensity ALK immunohistochemistry had a strong association with overexpression of ALK by Nanostring analysis.

Conclusions: ALK overexpression was extremely common in MCC by IHC and Nanostring analysis revealed that this was primarily due to WT-ALK expression and not ALK-fusions or the ALK-ATI. These findings may have therapeutic implications for the treatment of MCC.

500 Comparative Analysis of SNP Array and FISH in a Series of Ambiguous Melanocytic Lesions

Kabeer Shah[1], Ruifeng Guo[1], Lori Erickson[2], William Sukov[1], Thomas Flotte[2], Katherine Geiersbach[2]
[1]Rochester, MN, [2]Mayo Clinic, Rochester, MN

Disclosures: Kabeer Shah: None; Ruifeng Guo: None; Lori Erickson: None; William Sukov: None; Thomas Flotte: None; Katherine Geiersbach: None

Background: Ambiguous melanocytic lesions are rare; however, these lesions can pose challenging diagnostic dilemmas. Single nucleotide polymorphism chromosomal microarray (SNParray) and fluorescence in situ hybridization (FISH) have been recently utilized to interrogate copy number changes detected in malignant melanoma and to a lesser extent also detected in benign melanocytic lesions. However, there are limited data regarding the comparative performance of SNParray and FISH on ambiguous melanocytic lesions.

Design: DNA samples extracted from 101 formalin fixed, paraffin embedded melanocytic skin lesions with ambiguous histologic features were analyzed using the Affymetrix Oncoscan V3 SNP array platform. The anticipated FISH results were generated from the array raw data based on knowledge of FISH probe genomic coordinates and validated FISH reporting criteria, with the following assumptions: 1) tumor content was adequate given ≥40% tumor cellularity; 2) clinically relevant copy number variants affected the entire tumor cell population; 3) FISH analysis would have yielded accurate results.

Results: 101 ambiguous melanocytic lesions (median age 30.6 years, age range: 1.5-86 years) were analyzed by SNParray. Results included 93 losses, 51 gains, and 14 regions of copy neutral loss of heterozygosity (cnLOH) affecting clinically significant genes (including CDKN2A, BAP1, and TP53). In addition, copy number alterations with breakpoints in kinase genes were a recurrent finding in lesions with Spitzoid morphology. 50 cases (49.5%) had at least one chromosomal abnormality detected by SNParray. Of those lesions with a single abnormality, 10 (20%) would have yielded abnormal results by FISH. In accordance with previously proposed criteria for interpreting array data, 29 cases (28.7%) had ≥3 chromosomal abnormalities by SNParray, and only 10 of those 29 cases (34.5%) would have yielded abnormal results by FISH. SNP array thus increased the abnormality rate dramatically and also generated 21 equivocal results that did not meet proposed abnormal reporting criteria.

Conclusions: Clinical use of SNParray is challenging due to a lack of significant published data as seen with FISH. SNParray provides an expanded chromosomal landscape, including both copy number alterations and cnLOH, which can aid in distinguishing the biologic behavior of certain ambiguous melanocytic lesions.The use of SNParray technology detects the abnormalities detected by FISH but an increased number with significant chromosomal abnormalities.

501 Prevalence of Delta-like Protein 3 Expression in Merkel Cell Carcinoma

Wonwoo Shon[1], David Frishberg[2], Bonnie Balzer[3]
[1]Cedars-Sinai Medical Center, Studio City, CA, [2]Cedars-Sinai Medical Center, West Hollywood, CA, [3]Cedars-Sinai Medical Center, Los Angeles, CA

Disclosures: Wonwoo Shon: None; David Frishberg: None; Bonnie Balzer: None

Background: Merkel cell carcinoma (MCC) is an aggressive cutaneous neuroendocrine neoplasm. The majority of MCCs are associated with the oncogenic Merkel cell polyomavirus (MCPyV). Rovalpituzumab tesirine (Rova-T) is a first-in-class antibody-drug conjugate directed against delta-like protein 3 (DLL3) and has been shown to be a promising targeted therapy for tumors with neuroendocrine differentiation. We herein evaluate the expression of DLL3 in MCC by immunohistochemistry in order to evaluate its frequency and relation to MCPyV status.

Design: A total of 51 MCC cases were evaluated by tissue microarray. Immunohistochemistry was performed using monoclonal antibodies for DLL3 (SP347). The extent of cytoplasmic or membranous staining at any intensity was scored as those adopted in the phase I clinical trial of Rova-T (negative=<1%, low= 1?49%, and high= ?50%). In addition, all tumors were also stained with CM2B4 to measure MCPyV large T-antigen expression.

Results: DLL3 expression was observed in 48/51 (94%) MCC cases (DLL3-high: 31 cases and DLL3-low: 17 cases). 39/51 (76%) cases were positive for CM2B4. DLL3 expression was seen in all (100%) MCPyV-positive and 9/12 (75%) MCPyV-negative MCC (Table 1).

Table1. DLL3 expression in MCC by MCPyV status

	DLL3-negative	DLL3-low	DLL3-high	Total
MCPyV-positive	0	10	29	39
MCPyV-negative	3	7	2	12
Total	3	17	31	51

Conclusions: This is the first study to evaluate DLL3 expression in MCC. Although the exact function of DLL3 in MCC remains to be determined, the high prevalence of DLL3 expression in MCC suggests that it could be a therapeutic target for an antibody-drug conjugate Rova-T. Interestingly, DLL3 expression was not seen in a small subset of MCPyV-negative cases, possibly reflecting the different etiopathogenesis of MCC.

502 Quantification of 5-methylcytosine and 5-hydroxymethylcytosine in Cutaneous Squamous Cell Carcinoma of Organ Transplant Recipients

Wonwoo Shon[1], Mohammad Khan[2], Brian Cox[2], Bonnie Balzer[2]
[1]Cedars-Sinai Medical Center, Studio City, CA, [2]Cedars-Sinai Medical Center, Los Angeles, CA

Disclosures: Wonwoo Shon: None; Mohammad Khan: None; Brian Cox: None; Bonnie Balzer: None

Background: Solid organ transplant recipients have a high incidence of cutaneous squamous cell carcinoma (cSCC) and it is difficult to identify a high-risk subgroup. Accumulating data suggest that global loss of 5-hydroxymethylcytosine (5-hmC) is an epigenetic hallmark in different types of cancers and might play a critical role in tumor development and progression. Thus, in this study we investigate the status of 5-mC and 5-hmC in cSCC of organ transplant recipients.

Design: All available materials from 29 cSCC in patients with a known history of solid organ transplant were retrieved and re-reviewed. Follow-up was obtained. Formalin-fixed, paraffin-embedded whole tissue sections were immunostained for 5-mC and 5-hmC. Differences in 5-mC and 5-hmC expression among cSCC were assessed using Kruskal-Wallis H test.

Results: The patients with cSCC ranged in age from 57 to 99 years (mean, 70.2 years). Of the 29 patients, 23 patients were male and 6 were female. cSCC most often involved the head/neck. The expression of 5-hmC varied significantly among the different tumor grades ($p<0.001$). Diffuse loss of 5-hmC expression was seen in 10/11 poorly differentiated and 4/8 moderately differentiated cSCC. All well-differentiated tumors showed a strong and diffuse nuclear 5-hmC expression. However, the expression of 5-mC was statistically insignificant among the different tumor grades.

Conclusions: We determined that low 5-hmC expression was significantly associated with poor tumor grading in cSCC of organ transplant recipients. Because the loss of 5-hmC was not accompanied by a comparable decrease in 5-mC, it is conceivable that the loss of 5-hmC in cSCC reflects a defect in the Ten-Eleven Translocase mediated conversion. On-going analyses of additional clinical parameters should help to confirm the association between 5-mC/5-hmC expression and the biologic behavior of cSCC in the setting of post solid organ transplant.

503 Genotyping in Combination with Patient-derived Organotypic Tumor Modeling Indicates MAPK Pathway Alterations as a Therapeutic Target in Mucosal Melanoma.

Julia Thierauf[1], Stephanie Weissinger[2], Maciej Pacula[3], Valentina Nardi[3], Dora Dias-Santagata[3], Long Le[3], Elena-Sophie Prigge[4], Hans-Jürgen Stark[5], Magnus von Knebel Doeberitz[5], Cornelia Mauch[6], Christoph Bergmann[7], Annette Affolter[8], Thomas K. Hoffmann[9], Peter K. Plinkert[8], Jochen Hess[8], John Iafrate[3], Jochen Lennerz[10]
[1]Massachusetts General Hospital, Harvard Medical School, Heidelberg, Germany, [2]Institute of Pathology, University Hospital Ulm, Ulm, Germany, [3]Massachusetts General Hospital, Boston, MA, [4]University Hospital Heidelberg and German Cancer Research Center (DKFZ), Heidelberg, Germany, [5]University Hospital Heidelberg, German Cancer Research Center (DKFZ), Heidelberg, Germany, [6]University of Cologne, Cologne, Germany, [7]University Medical Center Essen, Essen, Germany,[8]Heidelberg University Hospital, Heidelberg, Germany, [9]University Medical Center Ulm, Ulm, Germany, [10]Massachusetts General Hospital, Harvard Medical School, Boston, MA

Disclosures: Julia Thierauf: None; Stephanie Weissinger: None; Valentina Nardi: None; Long Le: *Consultant*, ArcherDx; *Major Shareholder*, ArcherDx; Cornelia Mauch: None; John Iafrate: *Major Shareholder*, ArcherDx; Jochen Lennerz: None

Background: Mucosal melanoma (MM) is an aggressive malignancy without effective systemic therapies. Recent studies indicate the importance of MAPK pathway alterations and clinical trials with new MEK-inhibitors targeting activating NRAS and NF1 mutations are underway. However, given the overall rarity of MM, the challenges of genotype-driven trials are clear and patient-derived primary tumor model systems are one possibility to gain insight into therapeutic relevance of pathway alterations in MM. To our knowledge, integration of comprehensive panel sequencing results with preclinical sensitivity data is currently missing. Here we assessed the prevalence of MAPK alterations and feasibility of a prospective preclinical tumor model of MM.

Design: In a series of 60 cases, we analyzed the mutational landscape using anchored multiplex PCR (AMP) in combination with next-generation sequencing for 92 oncologically relevant genes including BRAF/NRAS/NF1. We established a prospective program to harvest and grow MM in a specific 3D-organotypic co-culture model (3D-MM-OTC). We performed immunohistochemistry for HMB-45, Melan-A, S100, and ki-67 to confirm melanocytic differentiation and proliferation in the co-culture model.

Results: Results: A total of 32 cases showed at least one alteration (53%) and a total of n=82 alterations were detected. Eighteen out of 60 patients (30%) harbored alterations in genes affecting the MAPK pathway. Overall, 14 MM samples from two different patients were grown on dermal equivalents reinforced by a scaffold of modified viscose fibers (non-woven Bemcot-M3) and colonized with skin fibroblasts, producing genuine dermis-type matrix. 3D-MM-OTC-models were successfully cultivated for up to 40 days (median: 21 days; range: 7-40 days). The MM cells showed migrating and proliferative activity that commenced a few days after tumor cells were placed on top of the dermal equivalents (Figure 1). Outgrowing cells expressed mucosal melanoma markers such as HMB-45, Melan-A and S100 equivalent to the primary tumor on day 0 and to mucosal melanoma in vivo.

Figure 1 - 503

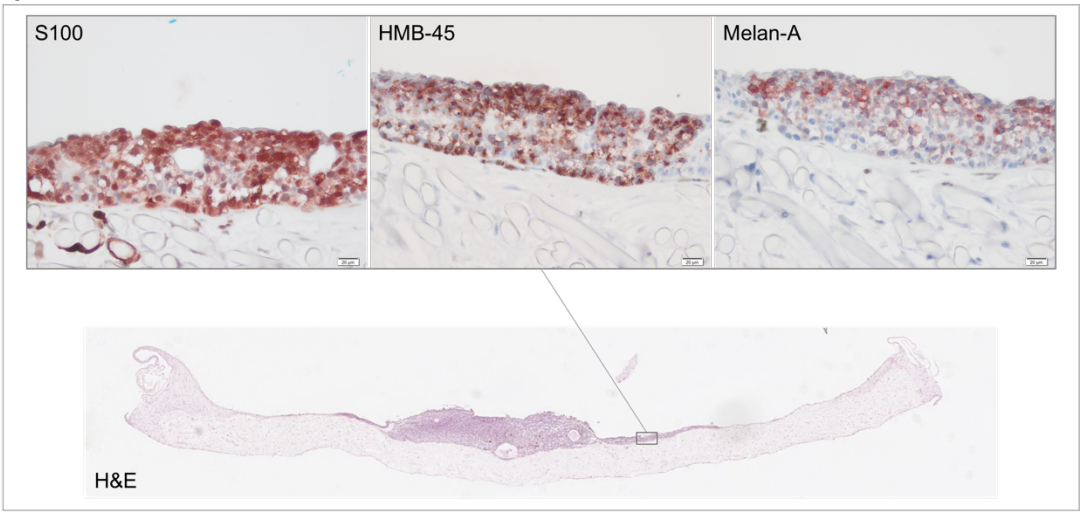

Figure 1. Formation of tumor cell layers after 21 days in culture with protein expression of S100, HMB-45 and Melan-A assessed by immunohistochemistry.

Conclusions: While genotyping of patient-derived organotypic tumor models is underway, the ability to concurrently assess genotype and establish a functional laboratory model enables a direct insight into the biology of this aggressive malignancy via interference with therapeutically relevant pathway alterations.

504 Next Generation of Immune Targets: CD47 and CD70 Expression in Cutaneous Lesions

Christopher Trindade[1], Tanupriya Agrawal[2], Saber Tadros[3], Patricia Fetsch[2], TaShanda Ashford[2], Abhik Ray-Chaudhury[4], Sara Peters[5], Armando Filie[2], Markku Miettinen[3], Stephen Hewitt[3]
[1]NIH/NCI/CCR/LP, Bethesda, MD, [2]National Institutes of Health/National Cancer Institute, Bethesda, MD, [3]National Cancer Institute, Bethesda, MD, [4]National Institutes of Health, Bethesda, MD, [5]The Ohio State University Wexner Medical Center, Columbus, OH

Disclosures: Christopher Trindade: None; Tanupriya Agrawal: None; Saber Tadros: None; Patricia Fetsch: None; TaShanda Ashford: None; Abhik Ray-Chaudhury: None; Sara Peters: None; Armando Filie: None; Markku Miettinen: None; Stephen Hewitt: None

Background: Checkpoint inhibitors such as PD-1 and PDL-1 have become a mainstay of therapy for cutaneous skin lesions such as melanoma and merkel cell carcinoma highlighting the promise and success of immunotherapy for skin tumors. Some patients, however, remain refractory to treatment and others will relapse and thus new targets that can modulate the tumor immune microenvironment are needed. Recently it has been shown that tumors can aberrantly express CD47 and CD70. Mechanisms for immune resistance include for CD47, activation of the SIRP (alpha) pathway that inhibits macrophage engulfment and for CD70 activation of T-regulatory cells and downregulation of effector T-cells. Information on expression in cutaneous lesions is lacking for both CD47 and CD70. Here we created a new simplified immunohistochemical scoring systems for both CD47 and CD70. Using tissue microarrays we analyzed expression in various benign and malignant skin lesions.

Design: Tissue microarrays included 600 formalin fixed paraffin embedded specimens from primary and metastatic cutaneous lesions including melanoma and squamous, basal, and merkel cell carcinoma obtained from NIH, University of Virginia, and Biomax (Rockville, MD). Some of the specimens included clinical information such as stage/progression and histological grade as wells as blocks, allowing for further investigation. After antibodies were validated a scoring system was developed for CD47 (Sigma, St. Louis, MO) and CD70 (R&D, Minneapolis, MN). For CD47, score 0- no stain, score 1- cytoplasmic/ weak membranous, score 2- moderate membranous, score 3- strong membranous. For CD70, score 0-no stain, score 1- cytoplasmic, score 2- golgi/weak membranous, score 3- strong membranous. Further investigation allowed us to look CD4, CD8, CD27, CD68, FoxP3, PD1, and PDL-1 in both strongly positive and negative skin lesions.

Results: In squamous cell carcinoma approximately 26% of CD47 and 20% of CD70 had a score of 2 or 3. In melanoma 9% of CD47 and 5% of CD70 had a score of 2 or 3. In basal cell carcinoma 22% of CD47 and 10% of CD70 had a score of 2 or 3. In merkel cell carcinoma 19% of CD70 had a score of 2 or 3. Differences were seen in strongly positive and negative CD47 and CD70 specimens.

Conclusions: A considerable number of cutaneous lesions were strongly positive for CD47 and CD70 in patient's specimens and may benefit from targeted therapy with clinical trials currently enrolling against both targets at the NIH.

505 Expression of PD-L1 and PD-1 in Cutaneous Warts

Wesley Yu[1], Timothy Berger[1], G. Zoltan Laszik[1], Jeffrey North[1], Jarish Cohen[1]
[1]University of California, San Francisco, San Francisco, CA

Disclosures: Wesley Yu: None; G. Zoltan Laszik: None; Jarish Cohen: None

Background: Cutaneous warts, also known as verrucas, are extremely common. Although they are considered benign, warts cause significant morbidity and are a substantial cost to the healthcare system. Despite multiple available treatment modalities, a sizeable number of warts remain resistant to numerous therapies. The human papilloma viruses (HPV) are the etiologic agents that cause verrucas. During the establishment of warts, HPV is thought to escape detection by the immune system, but the mechanisms that underlie this process are not completely understood. Given that a subset of warts demonstrates remarkable resistance to a variety of treatments, a possible mechanism for this phenomenon may be the induction of immune inhibitory molecules such as PD-L1 and dysfunction of PD-1-expressing lymphocytes.

Design: 22 biopsies of cutaneous warts including 15 biopsies of verruca vulgares and 7 biopsies of myrmecia (volar verrucas) were retrieved. Slides were stained with hematoxylin and eosin, anti-PD-L1 monoclonal antibody, and inflamed cases were stained with anti-PD-1 monoclonal antibody. Percentage of PD-L1-positive epithelial and inflammatory cells, percentage of PD-1-positive inflammatory cells, and quality/severity of the inflammatory infiltrate were evaluated.

Results: Patients ranged in age from 4 to 89 years old (median: 46) and gender (12/22, 55% female). PD-L1 was expressed on keratinocytes in 40% (6/15) of verruca vulgares and 43% (3/7) of myrmecia biopsies, and was associated with an interface inflammatory reaction. In cases that showed significant inflammation, PD-L1 was expressed on immune cells in 85% (11/13) of verruca vulgares and 100% (4/4) of myrmecia biopsies. Additionally, PD-1 was expressed by the inflammatory infiltrate in 85% (11/13) of verruca vulgares and 75% (3/4) of myrmecia biopsies.

Conclusions: A significant subset of cutaneous warts expresses PD-L1, suggesting that HPV utilizes this pathway to promote immune dysfunction. Upregulation of PD-L1 and concomitant expression of PD-1 on lymphocytes suggests a mechanism for the recalcitrance of some warts to current therapies, and provides a rationale for utilizing anti-PD-1 immunotherapy as a potential treatment for warts.